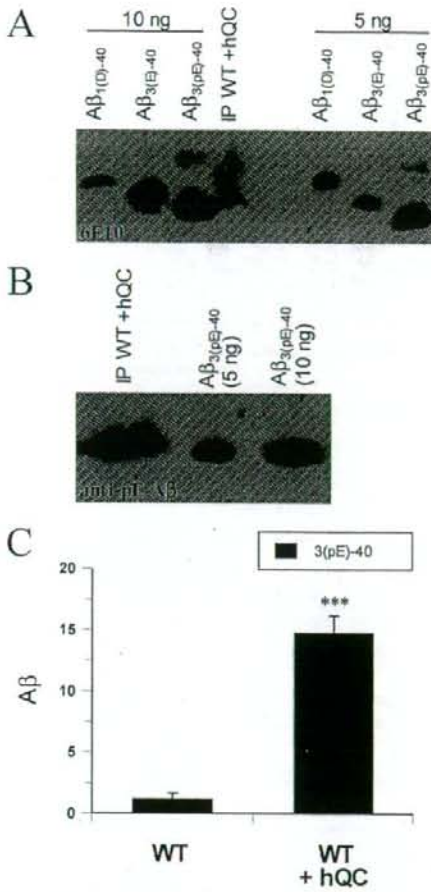

FIGURE 6: QC-dependent pGlu formation of APP(WT) was investigated by Western blotting after immunoprecipitation of Aβ peptides (application in comparison to standard Aβ peptides) using antibody 6E10, detecting total-Aβ (A) and antibody detecting pGlu-modified Aβ (B). (C) QC-dependent pGlu formation investigated using an ELISA after concentration of Aβ-containing cell media using centrifugal devices [single transfection of APP(WT) or cotransfection of APP(WT) with hQC] (Aβ concentration in picograms per milliliter) (asterisks, $P < 0.001$; Student's t test; $n = 5$).

LNZ308 cells (Figure 5C,D). The cell culture medium was analyzed for potential $A\beta_{3(pE)-40}$ formation. Intriguingly, the expression of APP variants containing the N3Q mutation led only in the case of APP(WT) and APP(London) to significant amounts of $A\beta_{3(pE)-40}$, whereas the presence of the Swedish mutation resulted only in scarce amounts of $A\beta_{3(pE)-40}$. This result was also observed when $A\beta_{3(pE)-42}$ was analyzed, pointing to differences in the liberation of Aβ peptides from APP molecules bearing the APP(WT) and APP(Swedish) sequence at the β-secretase cleavage site.

These significant differences in the liberation of N-truncated Aβ peptides prompted us to investigate the formation of $A\beta_{3(pE)}$ from APP(WT). As described for the APP(NLE) construct, cotransfection of APP(WT) and human QC was implemented to facilitate the formation of $A\beta_{3(pE)}$. On the basis of the urea−PAGE Western blot analysis, two different Aβ forms were detected (Figure 6A). The lower band corresponds to $A\beta_{3(pE)-40}$, whereas the upper band migrates slower than $A\beta_{1(D)-40}$, again suggesting an N-terminus differing from that of full-length Aβ, observed for APP(WT) expression. In addition, the results obtained by IP−Western blot analysis were validated by application of a pGlu-specific antibody (Figure 6B) and by concentration of the supernatant in centrifugal devices, followed by an ELISA, revealing significant $A\beta_{3(pE)-40}$ formation after cotransfection of APP(WT) and human QC (Figure 6C).

DISCUSSION

The Aβ peptides of amyloid deposits in brains of patients with Alzheimer's disease display a profound N- and C-terminal heterogeneity (*7, 11, 29*). Cleavage of γ-secretase causes primarily the C-terminal differences. Because neuritic plaques are mainly composed of $A\beta_{42}$, and the deposition of $A\beta_{42}$ precedes that of $A\beta_{40}$, $A\beta_{42}$ is thought to be more amyloidogenic than $A\beta_{40}$ (*27, 30*). The role and formation of N-terminal modifications, however, are more poorly understood. In particular, it is known that truncated Aβ peptides possessing a pGlu residue at the N-terminus are highly abundant in affected brains of patients with Alzheimer's disease and Down syndrome (*11, 12, 14*). Furthermore, the amyloidogenic peptides ABri in familial British dementia (FBD) and ADan in familial Danish dementia (FDD) possess an N-terminal pGlu residue, and pGlu formation appears to be crucial for the deposition of the ADan peptides in vivo (*31, 32*). Moreover, these pGlu-modified peptides have been shown to seed the aggregation of $A\beta_{1(D)-42}$ (*17*). Therefore, the prevention of pGlu formation might represent a new concept for the causal treatment of Alzheimer's disease and other pGlu-related amyloidoses.

However, the generation of pGlu peptides in AD, FBD, and FDD remained elusive, leaving room for speculation about their generation. In addition, despite evidence of an early role of pGlu-Aβ in the development of Alzheimer's disease, the formation of pGlu-Aβ peptides is frequently considered as a spontaneous secondary reaction occurring late in the progression of the disease (*33*). It should be noted that the uncatalyzed cyclization of N-terminal glutamic acid occurs exceptionally slowly, with half-lifes of years to decades under in vivo conditions (*43, 44*). In addition, since Aβ anabolism and catabolism make up a homeostasis showing a high rate of daily turnover, it is conceivable to assume an enzyme-catalyzed formation of pGlu-Aβ peptides. On the basis of artificial peptide substrates, recent in vitro studies provided the first evidence that glutamate cyclization at the N-terminus of Aβ might be due to catalysis of QC (*21, 22*). These results are highlighted here by the proof that the formation of $A\beta_{3(pE)-40/42}$ from glutamate occurs after amyloidogenic processing of APP. Most importantly, we describe for the first time the generation of $A\beta_{3(pE)}$ after expression of APP(WT), which is present in the vast majority of all AD cases, substantiating the assumption that QC might be a novel drug target for the treatment of pGlu-related amyloidoses.

According to the previous investigations of substrate specificity, the QC-catalyzed cyclization of glutamate requires a protonated γ-carboxyl group and an unprotonated α-amino group. The highest concentrations of these species are found under mildly acidic conditions around pH 6.0 (*21*). Similar pH conditions have been described for the secretory compartments

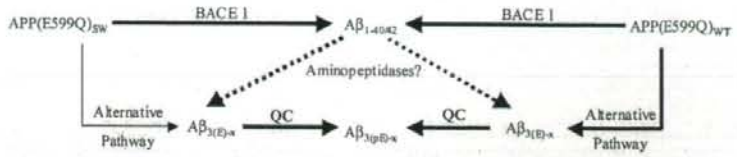

FIGURE 7: Proposed mechanism for the generation of N-terminally truncated Aβ peptides. Aβ is naturally liberated by N-terminal proteolysis due to BACE I, leading to $A\beta_{1(D)\text{-}40/42}$. This full-length Aβ species can be truncated by aminopeptidases. However, significant differences were observed for the generation of $A\beta_{3(pE)\text{-}x}$ between $APP(E599Q)_{WT}$ and $APP(E599Q)_{SW}$. Obviously, an alternative pathway exists, which is more pronounced for the $APP(E599Q)_{WT}$ variant. This leads to the generation of N-truncated $A\beta_{3(E)\text{-}x}$ species, which can be further cyclized by QC to obtain $A\beta_{3(pE)\text{-}x}$. Whether the alternative pathway represents different subcellular sites of BACE I-mediated Aβ liberation or a BACE I-independent mechanism has to be further addressed.

(*37*). As summarized in Figure 4, APP and QC are colocalized at least within the Golgi complex, where a spatially high concentration of both QC and Aβ or the respective β-CTFs can be expected (*34–36*). In this regard, these data suggest that the colocalization of QC and Aβ enhances pGlu-Aβ formation (Figure 3) and further support a catalyzed generation of this peptide species. In addition, the accumulation of pGlu-Aβ might also contribute to the intracellular aggregation of Aβ, which is frequently detected in patients with Down syndrome and Alzheimer's disease (*38–41*), in terms of generating the initial insoluble seeds for further Aβ deposition. The seeding capability of pGlu-Aβ was recently investigated in vitro, supporting the possibility that pGlu-Aβ can initiate seeding of full-length Aβ peptides (*17*).

Although these results strongly imply a QC-catalyzed formation of $A\beta_{3(pE)}$, a molecular pathway of APP processing leading finally to the substrate $A\beta_{3(E)\text{-}x}$ has never been investigated in detail. To examine the generation of $A\beta_{3(pE)}$ from APP processing, we introduced a novel monitoring mutation [APP(E599Q)], which leads to instant pGlu formation following the release of the N-terminal amino acids of Aβ. Intriguingly, the results suggest that the WT sequence at the β-secretase cleavage results in the production of N-truncated Aβ species, whereas the Swedish mutation leads preferentially to full-length $A\beta_{1(D)\text{-}x}$ peptides (Figure 7). Apparently, the endoproteolytic processing of APP(WT) and APP(Swedish) by β-secretase differs not only in our analyzed model system. Data from studies in transgenic animals overexpressing the APP(Swedish) mutation, e.g., Tg2576, have revealed conspicuous differences with regard to the Aβ composition (*42*). AD patients display up to 50% of pGlu-Aβ deposited as an early Aβ species. These mouse models, in stark contrast, show only minor amounts of pGlu-Aβ [up to 0.5% (unpublished data)] occurring late in the life span of Tg2576 (12−15 months of age) (S. Schilling et al., manuscript in preparation). Most intriguingly, Tg2576 shows only mild, if any, cognitive deficits, whereas animal models accumulating larger amounts of pGlu-Aβ display strong cognitive decline and hippocampal neuron loss (*20*).

In conclusion, the data presented here provide for the first time evidence that (i) cyclization of glutamic acid generating $A\beta_{3(pE)\text{-}40/42}$ is facilitated by QC after amyloidogenic processing of APP, (ii) the localization of QC and APP and the significant formation of $A\beta_{3(pE)\text{-}40/42}$ after coexpression point to a primarily intracellular pGlu generation, and (iii) the generation of N-truncated Aβ, accounting for the majority of Aβ in AD and DS, is possibly mediated by an alternative pathway of APP processing. The latter result is reflected in the unexpected finding of tremendous $A\beta_{3(pE)\text{-}40/42}$ formation in an APP(E599Q) variant, suggesting that the WT sequence at the β-cleavage site leads to Aβ molecules that are prone to cyclization by QC (Figure 7).

The results thus strongly imply that the majority of the pGlu peptides deposited in AD and DS brains are formed by enzymatic catalysis following processing of APP(WT). QC activity, mediated by the neurotoxic potential of $A\beta_{3(pE)\text{-}40/42}$, might be involved in the first intracellular events of the amyloid cascade, potentially driving the aggregation process of Aβ. The enhanced aggregation propensity and stability of pyroglutamated Aβ, in turn, might trigger the aggregation of other Aβ species, which are generated by β- and γ-secretase at higher levels. Accordingly, the prevention of pGlu-Aβ formation might represent a novel concept for a causal treatment of Alzheimer's disease.

ACKNOWLEDGMENT

We thank Dr. Torsten Hoffmann for helpful discussion and Anett Stephan for technical assistance. We also thank Dr. Steffen Rossner (Paul-Flechsig Institut for Brain Research, Leipzig, Germany) for the access to the laser-scanning microscope. The help of Jan Eggert in critically reading the manuscript is also gratefully acknowledged.

REFERENCES

1. Saido, T. C., and Iwata, N. (2006) Metabolism of amyloid β peptide and pathogenesis of Alzheimer's disease. Towards presymptomatic diagnosis, prevention and therapy. *Neurosci. Res. 54*, 235–253.
2. Selkoe, D. J. (2001) Alzheimer's disease: Genes, proteins, and therapy. *Physiol. Rev. 81*, 741–766.
3. Esler, W. P., and Wolfe, M. S. (2001) A portrait of Alzheimer secretases: New features and familiar faces. *Science 293*, 1449–1454.
4. Haass, C., Schlossmacher, M. G., Hung, A. Y., Vigo-Pelfrey, C., Mellon, A., Ostaszewski, B. L., Lieberburg, I., Koo, E. H., Schenk, D., Teplow, D. B., and Selkoe, D. J. (1992) Amyloid β-peptide is produced by cultured cells during normal metabolism. *Nature 359*, 322–325.
5. El Mouedden, M., Vandermeeren, M., Meert, T., and Mercken, M. (2006) Reduction of Aβ levels in the Sprague Dawley rat after oral administration of the functional γ-secretase inhibitor, DAPT: A novel non-transgenic model for Aβ production inhibitors. *Curr. Pharm. Des. 12*, 671–676.
6. Saido, T. C. (1998) Alzheimer's disease as proteolytic disorders: Anabolism and catabolism of β-amyloid. *Neurobiol. Aging 19*, S69−S75.
7. Saido, T. C., Yamao-Harigaya, W., Iwatsubo, T., and Kawashima, S. (1996) Amino- and carboxyl-terminal heterogeneity of β-amyloid peptides deposited in human brain. *Neurosci. Lett. 215*, 173–176.
8. Sergeant, N., Bombois, S., Ghestem, A., Drobecq, H., Kostanjevecki, V., Missiaen, C., Wattez, A., David, J. P., Vanmechelen, E., Sergheraert, C., and Delacourte, A. (2003) Truncated β-amyloid peptide species in pre-clinical Alzheimer's disease as new targets for the vaccination approach. *J. Neurochem. 85*, 1581–1591.
9. Jarrett, J. T., Berger, E. P., and Lansbury, P. T., Jr. (1993) The carboxy terminus of the β amyloid protein is critical for the seeding

of amyloid formation: Implications for the pathogenesis of Alzheimer's disease. *Biochemistry 32*, 4693–4697.
10. Roher, A. E., Palmer, K. C., Yurewicz, E. C., Ball, M. J., and Greenberg, B. D. (1993) Morphological and biochemical analyses of amyloid plaque core proteins purified from Alzheimer disease brain tissue. *J. Neurochem. 61*, 1916–1926.
11. Saido, T. C., Iwatsubo, T., Mann, D. M., Shimada, H., Ihara, Y., and Kawashima, S. (1995) Dominant and differential deposition of distinct β-amyloid peptide species, Aβ N3(pE), in senile plaques. *Neuron 14*, 457–466.
12. Russo, C., Saido, T. C., DeBusk, L. M., Tabaton, M., Gambetti, P., and Teller, J. K. (1997) Heterogeneity of water-soluble amyloid β-peptide in Alzheimer's disease and Down's syndrome brains. *FEBS Lett. 409*, 411–416.
13. Russo, C., Salis, S., Dolcini, V., Venezia, V., Song, X. H., Teller, J. K., and Schettini, G. (2001) Amino-terminal modification and tyrosine phosphorylation of carboxy-terminal fragments of the amyloid precursor protein in Alzheimer's disease and Down's syndrome brain. *Neurobiol. Dis. 8*, 173–180.
14. Hosoda, R., Saido, T. C., Otvos, L., Arai, T., Mann, D. M., Lee, V. M., Trojanowski, J. Q., and Iwatsubo, T. (1998) Quantification of modified amyloid β peptides in Alzheimer disease and Down syndrome brains. *J. Neuropathol. Exp. Neurol. 57*, 1089–1095.
15. Harigaya, Y., Saido, T. C., Eckman, C. B., Prada, C. M., Shoji, M., and Younkin, S. G. (2000) Amyloid β protein starting pyroglutamate at position 3 is a major component of the amyloid deposits in the Alzheimer's disease brain. *Biochem. Biophys. Res. Commun. 276*, 422–427.
16. Russo, C., Violani, E., Salis, S., Venezia, V., Dolcini, V., Damonte, G., Benatti, U., D'Arrigo, C., Patrone, E., Carlo, P., and Schettini, G. (2002) Pyroglutamate-modified amyloid β-peptides—AβN3(pE)—strongly affect cultured neuron and astrocyte survival. *J. Neurochem. 82*, 1480–1489.
17. Schilling, S., Lauber, T., Schaupp, M., Manhart, S., Scheel, E., Bohm, G., and Demuth, H. U. (2006) On the seeding and oligomerization of pGlu-amyloid peptides (in vitro). *Biochemistry 45*, 12393–12399.
18. He, W., and Barrow, C. J. (1999) The Aβ 3-pyroglutamyl and 11-pyroglutamyl peptides found in senile plaque have greater β-sheet forming and aggregation propensities in vitro than full-length Aβ. *Biochemistry 38*, 10871–10877.
19. Piccini, A., Russo, C., Gliozzi, A., Relini, A., Vitali, A., Borghi, R., Giliberto, L., Armirotti, A., D'Arrigo, C., Bachi, A., Cattaneo, A., Canale, C., Torrassa, S., Saido, T. C., Markesbery, W., Gambetti, P., and Tabaton, M. (2005) β-Amyloid is different in normal aging and in Alzheimer's disease. *J. Biol. Chem. 280*, 34186–34192.
20. Casas, C., Sergeant, N., Itier, J. M., Blanchard, V., Wirths, O., van der, K. N., Vingtdeux, V., van de, S. E., Ret, G., Canton, T., Drobecq, H., Clark, A., Bonici, B., Delacourte, A., Benavides, J., Schmitz, C., Tremp, G., Bayer, T. A., Benoit, P., and Pradier, L. (2004) Massive CA1/2 neuronal loss with intraneuronal and N-terminal truncated Aβ42 accumulation in a novel Alzheimer transgenic model. *Am. J. Pathol. 165*, 1289–1300.
21. Schilling, S., Hoffmann, T., Manhart, S., Hoffmann, M., and Demuth, H. U. (2004) Glutaminyl cyclases unfold glutamyl cyclase activity under mild acid conditions. *FEBS Lett. 563*, 191–196.
22. Cynis, H., Schilling, S., Bodnar, M., Hoffmann, T., Heiser, U., Saido, T. C., and Demuth, H. U. (2006) Inhibition of glutaminyl cyclase alters pyroglutamate formation in mammalian cells. *Biochim. Biophys. Acta 1764*, 1618–1625.
23. Shirotani, K., Tsubuki, S., Lee, H. J., Maruyama, K., and Saido, T. C. (2002) Generation of amyloid β peptide with pyroglutamate at position 3 in primary cortical neurons. *Neurosci. Lett. 327*, 25–28.
24. Klafki, H. W., Wiltfang, J., and Staufenbiel, M. (1996) Electrophoretic separation of βA4 peptides (1−40) and (1−42). *Anal. Biochem. 237*, 24–29.
25. Schilling, S., Hoffmann, T., Wermann, M., Heiser, U., Wasternack, C., and Demuth, H. U. (2002) Continuous spectrometric assays for glutaminyl cyclase activity. *Anal. Biochem. 303*, 49–56.
26. Citron, M., Oltersdorf, T., Haass, C., McConlogue, L., Hung, A. Y., Seubert, P., Vigo-Pelfrey, C., Lieberburg, I., and Selkoe, D. J. (1992) Mutation of the β-amyloid precursor protein in familial Alzheimer's disease increases β-protein production. *Nature 360*, 672–674.
27. Suzuki, N., Cheung, T. T., Cai, X. D., Odaka, A., Otvos, L., Jr., Eckman, C., Golde, T. E., and Younkin, S. G. (1994) An increased percentage of long amyloid β protein secreted by familial amyloid β protein precursor (βAPP717) mutants. *Science 264*, 1336–1340.
28. Schilling, S., Hoffmann, T., Rosche, F., Manhart, S., Wasternack, C., and Demuth, H. U. (2002) Heterologous expression and characterization of human glutaminyl cyclase: Evidence for a disulfide bond with importance for catalytic activity. *Biochemistry 41*, 10849–10857.
29. Kuo, Y. M., Emmerling, M. R., Woods, A. S., Cotter, R. J., and Roher, A. E. (1997) Isolation, chemical characterization, and quantitation of Aβ 3-pyroglutamyl peptide from neuritic plaques and vascular amyloid deposits. *Biochem. Biophys. Res. Commun. 237*, 188–191.
30. Iwatsubo, T., Odaka, A., Suzuki, N., Mizusawa, H., Nukina, N., and Ihara, Y. (1994) Visualization of Aβ42(43) and Aβ40 in senile plaques with end-specific Aβ monoclonals: Evidence that an initially deposited species is Aβ42(43). *Neuron 13*, 45–53.
31. Tomidokoro, Y., Lashley, T., Rostagno, A., Neubert, T. A., Bojsen-Moller, M., Braendgaard, H., Plant, G., Holton, J., Frangione, B., Revesz, T., and Ghiso, J. (2005) Familial Danish dementia: Co-existence of Danish and Alzheimer amyloid subunits (ADan AND Aβ) in the absence of compact plaques. *J. Biol. Chem. 280*, 36883–36894.
32. Ghiso, J., Revesz, T., Holton, J., Rostagno, A., Lashley, T., Houlden, H., Gibb, G., Anderton, B., Bek, T., Bojsen-Moller, M., Wood, N., Vidal, R., Braendgaard, H., Plant, G., and Frangione, B. (2001) Chromosome 13 dementia syndromes as models of neurodegeneration. *Amyloid 8*, 277–284.
33. Hashimoto, T., Wakabayashi, T., Watanabe, A., Kowa, H., Hosoda, R., Nakamura, A., Kanazawa, I., Arai, T., Takio, K., Mann, D. M., and Iwatsubo, T. (2002) CLAC: A novel Alzheimer amyloid plaque component derived from a transmembrane precursor, CLAC-P/collagen type XXV. *EMBO J. 21*, 1524–1534.
34. Greenfield, J. P., Tsai, J., Gouras, G. K., Hai, B., Thinakaran, G., Checler, F., Sisodia, S. S., Greengard, P., and Xu, H. (1999) Endoplasmic reticulum and trans-Golgi network generate distinct populations of Alzheimer β-amyloid peptides. *Proc. Natl. Acad. Sci. U.S.A. 96*, 742–747.
35. Hartmann, T., Bieger, S. C., Bruhl, B., Tienari, P. J., Ida, N., Allsop, D., Roberts, G. W., Masters, C. L., Dotti, C. G., Unsicker, K., and Beyreuther, K. (1997) Distinct sites of intracellular production for Alzheimer's disease Aβ40/42 amyloid peptides. *Nat. Med. 3*, 1016–1020.
36. Fischer, W. H., and Spiess, J. (1987) Identification of a mammalian glutaminyl cyclase converting glutaminyl into pyroglutamyl peptides. *Proc. Natl. Acad. Sci. U.S.A. 84*, 3628–3632.
37. Demaurex, N., Furuya, W., D'Souza, S., Bonifacino, J. S., and Grinstein, S. (1998) Mechanism of acidification of the trans-Golgi network (TGN). In situ measurements of pH using retrieval of TGN38 and furin from the cell surface. *J. Biol. Chem. 273*, 2044–2051.
38. Gouras, G. K., Almeida, C. G., and Takahashi, R. H. (2005) Intraneuronal Aβ accumulation and origin of plaques in Alzheimer's disease. *Neurobiol. Aging 26*, 1235–1244.
39. Mori, C., Spooner, E. T., Wisniewsk, K. E., Wisniewski, T. M., Yamaguch, H., Saido, T. C., Tolan, D. R., Selkoe, D. J., and Lemere, C. A. (2002) Intraneuronal Aβ42 accumulation in Down syndrome brain. *Amyloid 9*, 88–102.
40. Gouras, G. K., Tsai, J., Naslund, J., Vincent, B., Edgar, M., Checler, F., Greenfield, J. P., Haroutunian, V., Buxbaum, J. D., Xu, H., Greengard, P., and Relkin, N. R. (2000) Intraneuronal Aβ42 accumulation in human brain. *Am. J. Pathol. 156*, 15–20.
41. Gyure, K. A., Durham, R., Stewart, W. F., Smialek, J. E., and Troncoso, J. C. (2001) Intraneuronal Aβ-amyloid precedes development of amyloid plaques in Down syndrome. *Arch. Pathol. Lab. Med. 125*, 489–492.
42. Kawarabayashi, T., Younkin, L. H., Saido, T. C., Shoji, M., Ashe, K. H., and Younkin, S. G. (2001) Age-dependent changes in brain, CSF, and plasma amyloid β protein in the Tg2576 transgenic mouse model of Alzheimer's disease. *J. Neurosci. 21*, 372–381.
43. Yu, L., Vizel, A., Huff, M. B., Young, M., Remmele, R. L., Jr., and He, B. (2006) Investigation of N-terminal glutamate cyclization of recombinant monoclonal antibody in formulation development. *J. Pharm. Biomed. Anal. 42*, 455–463.
44. Chelius, D., Jing, K., Lueras, A., Rehder, D. S., Dillon, T. M., Vizel, A., Rajan, R. S., Li, T., Treuheit, M. J., and Bondarenko, P. V. (2006) Formation of pyroglutamic acid from N-terminal glutamic acid in immunoglobulin γ antibodies. *Anal. Chem. 78*, 2370–2376.

BI800250P

Altered Function of Factor I Caused by Amyloid β: Implication for Pathogenesis of Age-Related Macular Degeneration from Drusen[1]

Jiying Wang,* Kyoko Ohno-Matsui,[2]* Takeshi Yoshida,* Ariko Kojima,* Noriaki Shimada,* Ken-ichi Nakahama,† Olga Safranova,† Nobuhisa Iwata,‡ Takaomi C. Saido,‡ Manabu Mochizuki,* and Ikuo Morita†

The results of recent studies have implicated local inflammation and complement activation as the processes involved in the pathogenesis of age-related macular degeneration (AMD). We have demonstrated that amyloid β (Aβ), which is deposited in drusen, causes an imbalance in the angiogenesis-related factors in retinal pigment epithelial cells. We have also shown that neprilysin gene-disrupted mice accumulate Aβ, and develop several features of AMD. The purpose of this study was to investigate the mechanisms involved in the development of AMD that are triggered by Aβ. Our results showed that Aβ binds to complement factor I which inhibits the ability of factor I to cleave C3b to inactivated iC3b. Factor H and factor I are soluble complement-activation inhibitors, and preincubation of factor I with Aβ in the presence of factor H abolished the ability of Aβ to cleave C3b, and also abolished the ability of factor I to cleave FGR-AMC. In contrast, Aβ did not affect the function of factor H even after binding. The production of iC3b was significantly decreased when C3b and factor H were incubated with the eyes from neprilysin gene-disrupted mice as compared with when C3b and factor H were incubated with eyes from age-matched wild-type mice. These results suggest that Aβ activates the complement system within drusen by blocking the function of factor I leading to a low-grade, chronic inflammation in subretinal tissues. These findings link four factors that have been suggested to be associated with AMD: inflammation, complement activation, Aβ deposition, and drusen. *The Journal of Immunology,* **2008, 181: 712–720.**

The complement system is a component of the humoral immune system involved in host defense, and it can be activated through three distinct pathways: the classical, the alternative, and the lectin. Activation of these three pathways leads to the cleavage of C3 into C3a and C3b (1), which finally leads to the formation of the C5b-9 membrane attack complex (MAC)[3] (1–3). The MAC is a lytic complex that is lethal not only to foreign pathogens but also to local host cells and tissues. Thus, the regulation of complement activation is important for the maintenance of tissue homeostasis and is mediated by a family of complement proteins.

There has recently been an increased interest in the involvement of complement in the development and progression of many diseases including age-related macular degeneration (AMD). AMD is the leading cause of irreversible vision loss, affecting 30~50 million elderly individuals worldwide (4–7). Two major clinical phenotypes of AMD are recognized: a nonexudative (dry) type and an exudative (wet) type. Recent studies have demonstrated that local and chronic inflammation induced by the complement pathway plays a central role in the formation of drusen and the development of AMD (8–11).

Polymorphisms in the genes coding for complement factor H and factor B have been shown to be predictors of the risk of developing AMD (12–17). Factor H and factor B are key components of the alternative complement pathway. Factor H, the most important soluble complement activation inhibitor, blocks the binding of factor B to C3b, supports the dissociation of the C3bBb complex (decay-accelerating activity), and acts as a cofactor in the cleavage of C3b by factor I (18, 19). Another susceptible locus for AMD is the hypothetical gene called *LOC387715/HTRA1* (17, 20–22). The population risk associated with variants of factor H, factor B, and *LOC387715/HTRA1* is at least 50% (17). In addition, a very recent study confirmed that functional polymorphisms in the *C3* gene were strongly associated with AMD (23). These genetic studies in patients with AMD, together with the finding that proteins associated with inflammation and immune-mediated processes are deposited in drusen and Bruch's membrane in eyes with AMD (24), support the hypothesis that inflammation and complement activation are involved in the pathogenesis of AMD. Also, animal experiments, using a laser-induced choroidal neovascularization model, showed that the activation of the complement alternative

*Department of Ophthalmology and Visual Science, Tokyo Medical and Dental University, Tokyo, Japan; †Section of Cellular Physiological Chemistry, Tokyo Medical and Dental University, Tokyo, Japan; and ‡Laboratory for Proteolytic Neuroscience, Institute of Physical and Chemical Research (RIKEN) Brain Science Institute, Wako-shi, Saitama, Japan

Received for publication November 13, 2007. Accepted for publication April 29, 2008.

The costs of publication of this article were defrayed in part by the payment of page charges. This article must therefore be hereby marked *advertisement* in accordance with 18 U.S.C. Section 1734 solely to indicate this fact.

[1] This work was supported in part by Research Grants 19390441, 18023037, and 19659445 from the Japan Society for the Promotion of Science, Tokyo, Japan. This work was supported in part by Grants-in-Aid for Scientific Research on Priority Areas, Research on Pathomechanisms of Brain Disorders 18023037 (to N.I.) and 20023031 (to N.I.) from the Ministry of Education, Culture, Sports, Science, and Technology, Japan.

[2] Address correspondence and reprint requests to Dr. Kyoko Ohno-Matsui, Department of Ophthalmology and Visual Science, Tokyo Medical and Dental University, 1-5-45 Yushima, Bunkyo-ku, Tokyo 113, Japan. E-mail address: k.ohno.oph@tmd.ac.jp

[3] Abbreviations used in this paper: MAC, membrane attack complex; AMD, age-related macular degeneration; RPE, retinal pigmented epithelium; Aβ, amyloid β; AD, Alzheimer's disease; FGF, fibroblast growth factor; FHL, factor H-like protein.

 0022-1767/08/$2.00

pathway was critical for the development of choroidal neovascularization (25), a major feature of the neovascular form of AMD.

One of the earliest clinical hallmarks of AMD is subretinal extracellular deposits, known as drusen, which accumulate beneath the retinal pigmented epithelium (RPE) (26). Epidemiological studies have shown that numerous and/or confluent drusen significantly increase the risk for the development of AMD (27, 28). However, the mechanism of the development of AMD from drusen has not been precisely determined. Recent proteomic analyses have shown that drusen contain many proteins, such as cholesterol, apolipoproteins B and E, C-reactive protein, clusterin, vitronectin, and amyloid β (Aβ) (24, 29, 30). Among these proteins, we focused on Aβ as the primary stimulus that causes the development of AMD (31).

Aβ peptides vary in length from 39- to 43-aa residues and are produced by the sequential proteolytic processing of amyloid precursor proteins. Studies have shown that Aβ is the main component of senile plaques in the brain of patients with Alzheimer's disease (AD), and the transition of Aβ from the monomeric form to the oligomeric or aggregated form in the brain is a key event in the pathogenesis of AD (32–34). The results of our earlier study demonstrated that exposure of RPE cells to Aβ induced a marked increase in vascular endothelial growth factor and a marked decrease of pigment epithelium-derived factor, an antiangiogenic factor, in the RPE cells (31). Importantly, there was an increase in the deposition of Aβ in the subretinal space of senescent neprilysin gene-disrupted mice, and these mice developed several features of human eyes with AMD (31). These results suggest that Aβ deposited in drusen may be a key contributor to the development of AMD. However, the underlying molecular mechanism on how Aβ leads to the features of AMD has not been determined.

The pathogenesis of AD has also been considered to be one of the inflammatory processes caused by complement activation (35). Aβ is colocalized with activated complement components, the C5b-9 MAC, in the brain of AD patients (36). Aβ activates the alternative pathway by triggering the formation of covalent, ester-linked complexes of Aβ with C3b/iC3b, an activation product of the third complement component (C3) (36). Also in AMD, Johnson et al. (29) demonstrated that Aβ is colocalized with the activation-specific fragments of complement C3 in unique substructural domains, the "amyloid vesicles," within the drusen thereby identifying them as potential sites of complement activation.

These findings led us to hypothesize that AMD results from an abnormal inflammatory process which includes an unregulated activation of the complement pathway triggered by Aβ, as suggested for AD. Although there has been a publication demonstrating the colocalization of complement proteins and Aβ in eyes with AMD (29), the precise mechanism of how complement is activated by Aβ in AMD has not been determined. Based on the human pathological studies and our previous animal experiments, we have explored the influence of Aβ on the activation of the alternative pathway, and we will present new evidence that Aβ binds and inactivates the function of complement factor I. This then results in an unregulated activation of complement in subretinal tissues.

Materials and Methods

Materials

DMEM, TRIzol reagent, and the SilverQuest silver staining kit were purchased from Invitrogen; plastic ware (Falcon) was obtained from BD Biosciences; FCS was obtained from HyClone; human recombinant basic fibroblast growth factor (FGF) was obtained from R&D Systems; laminin was obtained from Upstate Biotechnology; You-Prime First-Strand Beads, PCR beads, and nylon membranes were obtained from Amersham Pharmacia Biotech; agarose was obtained from Takara; $A\beta_{1-40}$ (HCl form) and $A\beta_{40-1}$ were obtained from Peptide Institute. The mAb against Aβ (4G8) was purchased from SIGNET; the iC3b ELISA kit, purified human factor H, and purified human factor I were obtained from Quidel; purified human C3b was obtained from Biogenesis; mAb against human factor I (MCA507, OX21), mAb against human factor H (MCA509, OX24), and polyclonal antiserum against human C3 (AHC007) were obtained from Serotec; recombinant substrate FGR-AMC was obtained from American Diagnostica; Microfluor white plates were obtained from Packard Bioscience; the0.4-μm pore-size transwell was obtained from Corning; the XTT cell proliferation assay kit was obtained from Cayman Chemical.

Human RPE cell cultures

Primary cultures of human RPE cells were a gift from Dr. P. A. Campochiaro (Wilmer Eye Institute, Johns Hopkins University, Baltimore, MD). The cultures used for the experiments were at the third or fourth passage at the time of separation. Cultures were shown to be pure populations of RPE cells by immunocytochemical staining for cytokeratins (data not shown). Differentiated RPE cells were established as described (37, 38). RPE cell cultures were maintained in DMEM supplemented with 10% FBS and 10 ng/ml basic FGF. The cells exhibited epithelial morphology and expressed CRALBP, a marker for differentiated RPE cells (38).

RPE cells were subcultured in 12-well tissue-culture plates at a density of 6×10^4 cells/well. Seven days after reaching confluence, the medium was changed, and cells were incubated in serum-free DMEM (500 μl) in the presence (50 μM) or absence of $A\beta_{1-40}$ peptide (HCl form). After 24 h, the medium was collected and stored at -20°C until use for Western blot analysis and ELISA. The cells were homogenized, and their RNA and protein were extracted. Each condition was examined in triplicate, and results were repeated in at least three independent experiments.

Cell viability assay

Seven days after reaching cellular confluence, the medium was changed, and cells were incubated in serum-free DMEM in the presence (25 or 50 μM) or absence of $A\beta_{1-40}$ peptide (HCl form) for 24 h. The XTT assay was used to measure viability using XTT reagent (Cayman Chemical), which was added for 1 h at 37°C and was quantified using an ELISA plate reader. The average absorbance measured for medium plus treatment was subtracted from each test sample. Each experiment was performed at least three times on different days.

RT-PCR for C3, C5, factor H, factor H-like protein (FHL), factor B, and factor I

Total RNA was extracted from cultured RPE cells using TRIzol reagent. cDNA was synthesized from 2 μg of total RNA using You-Prime First-Strand Beads according to the manufacturer's protocol, and the reaction products were subjected to PCR amplification using the GeneAmp PCR system (Cetus; PerkinElmer). The mRNAs of human C3, C5, factor H, FHL (a truncated form of factor H (39)), factor B, and factor I were amplified with the following primers: for C3 (40), 5′-TCACCGTCAACC ACAAGCTGCTACC-3′ (forward) and 5′-TTTCATAGTAGGCTCGGA TCTTCCA-3′ (reverse); for C5 (40), 5′-GTGGCATTAGCAGCAGTG GACAGTG-3′ (forward) and 5′-GCAGGCTCCATCGTAACAACATT TC-3′ (reverse); for factor H (41), 5′-TCTGCATGTTGGCCTTCCT GTC-3′ (forward) and 5′-CTTCCTTGTAAATCTCCACCTG-3′ (reverse); for FHL (40), 5′-CAGAAGTTCAGAGGGTAAAGCT-3′ (forward) and 5′-TACTGGCTGGATACCTGCTCCG-3′ (reverse); for factor B (42), 5′-CAACAGAAGCGGAAGATCGTC-3′ (forward) and 5′-TAT CTCCAGGTCCCGCTTCTC-3′ (reverse); and for factor I (43), 5′-GGC AGGTGGCAATTAAGGATG-3′ (forward) and 5′-GGTGTATCCAGT CTACTACTGT-3′·(reverse).

The PCR for factor H and FHL was repeated for 30 cycles, and each cycle included denaturation at 94°C for 1 min, annealing at 58°C for 1 min, and primer extension at 72°C for 1 min. The PCR for C3 and C5 was repeated for 30 cycles, and each cycle included denaturation at 94°C for 1 min, annealing at 62°C for 1 min, and primer extension at 72°C for 1 min. The PCR for factor I was repeated for 30 cycles, and each cycle included denaturation at 94°C for 1 min, annealing at 60°C for 1 min, and primer extension at 72°C for 1 min. The PCR for factor B was repeated for 35 cycles, and each cycle included denaturation at 94°C for 1 min, annealing at 59°C for 1 min, and primer extension at 72°C for 1 min. The expected size of the reaction products was 186 bp for C3, 315 bp for C5, 424 bp for FHL, 354 bp for factor H, 884 bp for factor B, and 146 bp for factor I.

LightCycler real-time PCR

The cDNA was subjected to quantitative PCRs on a LightCycler Instrument (Roche Diagnostics) using the QuantiTect SYBR Green PCR kit (Qiagen) for C3, factor H, and factor I. PCR amplifications were performed

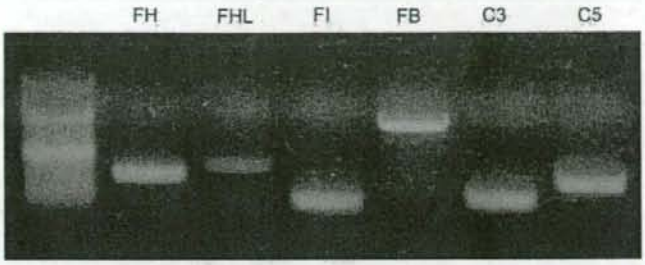

FIGURE 1. RT-PCR detection of complement proteins and their regulators in cultured human RPE cells. Human RPE cells were cultured in DMEM containing 10% FCS and 10 ng/ml basic FGF. After attaining confluence, total RNA was extracted from cultured RPE cells. cDNAs were synthesized from 2 μg of total RNA, and the reaction products were subjected to PCR amplification using specific primers for each factor. FH, Factor H; FI, factor I; FB, factor B.

with specific primers in a total volume of 20 μl containing 2 μl of sense and antisense primer mixture (0.5 μM of each primer), 10 μl of 2× SYBR Green QPCR Master Mix (Qiagen), 1 μl of 1/10 diluted cDNA, and 7 μl of nuclease-free PCR-grade water. The mixture was used as a template for the amplification after initial denaturation at 95°C and 40~50 cycles (95°C for 10 s, 58~62°C for 15 s, and 72°C for 30 s). The primer sequences of human GAPDH were 5′-ACCACAGTCCATGCCATCAC-3′ (forward) and 5′-TCCACCACCCTGTTGCTGTA-3′ (reverse). The primer sequences of C3, factor H, factor B, and factor I were the same as used for semiquantitative RT-PCR. SYBR Green fluorescence was measured, and quantification of each PCR product was expressed relative to GAPDH.

ELISA measurements of C3 fragments

The amount of iC3b secreted from RPE cells into the conditioned medium was determined with a commercial ELISA kit according to the manufacturer's instructions. The absorbance was measured at 405 nm in a Bio-Rad Model 450 microplate reader. Serial dilutions of recombinant C3 and iC3b were measured and a standardized curve was constructed.

Five days after cellular confluence, the medium was changed to serum-free DMEM. Then, the cells were incubated with or without $A\beta_{1-40}$ (HCl form; 50 μM) or $A\beta_{40-1}$ for 24 h. In some experiments, exogenous C3b (5 μg/ml) was added to the medium, and in other experiments, cells were preincubated with or without $A\beta_{1-40}$ (HCl form; 50 μM) for 12 h. After the preincubation, C3b (5 μg/ml) and various concentrations of purified human factor H or factor I were added to the medium. The conditioned media were collected after another 12 h, and the amount of iC3b was measured.

For transwell membrane experiments, cultured RPE cells were seeded onto cell culture inserts (0.4-μm pore size; Costar; Corning). Five days after cellular confluence, the medium was changed to serum-free DMEM. In this experiment, the exogenous C3b and $A\beta_{1-40}$ were added into the lower chamber. The conditioned media were also collected from the lower chamber.

Because it has already been reported that mouse complement factor I can cleave human C3b in the presence of human complement factor H (44), the ability of cleaving human C3b by the eye samples from both 12-mo-old neprilysin gene-disrupted mice (which leads to an increased deposition of Aβ as we demonstrated previously (31)) and age-matched wild-type mice was examined. Briefly, eyes were enucleated and the anterior segment as well as the neural retina was removed from the eyecup before sclera and the vascular choroid were carefully removed as much as possible using forceps. Electron microscopic examination confirmed that the intact RPE-Bruch's membrane-choriocapillaris complex and only a small amount of vascular choroid were removed in preliminary experiments (data not shown). The RPE-Bruch's membrane-choriocapillaris complex was pooled from four eyes, respectively, from wild-type or neprilysin gene-disrupted mice, and then were transferred into 1.5-ml assay tubes containing 40 μl of 10 μM phosphate buffer (pH 7.4; containing 145 mM NaCl) including 3.2 μg of human C3b and 3.2 μg of human factor H. The mixtures were centrifuged and incubated at 37°C for 12 h before being submitted to human iC3b EIA.

Western blot analyses

For the Western blot analysis of C3, factor H, and factor I, RPE cells were maintained in serum-free medium for 24 h; the conditioned media were collected and cells were lysed in 1 ml of sample buffer (125 mM Tris-HCl (pH 6.8), 2% SDS, 5% glycerol, 0.003% bromphenol blue, and 1% 2-ME). The final protein concentration was determined using a BCA assay (Pierce) according to the manufacturer's instructions. Equal amounts of secreted protein (8 μg) or a sample of the whole cell lysate (80 μg) were separated by 8% SDS-PAGE and electrophoretically transferred onto nylon membranes. The nylon membranes containing the transferred proteins were pretreated with 5.0% nonfat dried milk in 50 mM Tris (pH 8.0) and then incubated overnight with a monoclonal Ab against human C3 (1/1000 dilution), mAb against human factor H (1/200 dilution), or mAb against human factor I (1/200 dilution). SDS-PAGE analysis for C3, factor H, and factor I was performed under nonreduced conditions.

Measurement of factor I cofactor activity

The cleavage of C3b by factor I in the presence of factor H was performed in 10 mM phosphate buffer (pH 7.4) containing 145 mM NaCl, according to the method of Sahu et al. (45) In a typical assay, C3b (80 ng/μl), factor H (80 ng/μl), and factor I (3.5 ng/μl) were mixed in 10 μM phosphate buffer (pH 7.4; containing 145 mM NaCl). The total volume in each reaction tube was adjusted to 20 μl, and the tube was incubated at 37°C. In some experiments, factor I and/or factor H were preincubated with $A\beta_{1-40}$ (200 μM) for 1 h, and then incubated with C3b. After another 1 h, samples (5 μl) were removed and mixed with sample buffer containing DTT, boiled for 5 min, and subjected to electrophoresis on an 8% SDS-PAGE gel. The cleavage products were made visible by silver staining of the gel.

Amidolytic assay using synthetic substrate

The cleavage of the synthetic FGR-AMC by factor I in the presence or absence of Aβ was examined. This substrate is cleaved by factor I in the absence of any cofactors (46). FGR-AMC (50 μM; final concentration) in 20 mM HEPES at pH 8.5 was added to factor I (0.5 μM; final concentration) in the same buffer in a white Microfluor plate. The final reaction volume was 200 μl. The reaction was performed in the presence or absence of $A\beta_{1-40}$ (200 μM, final concentration). The amidolytic activity of factor I was measured using a microtiter plate reader (Fluoroskan; Thermo Life Sciences) by excitation at 355 nm and continuous monitoring of emission at 460 nm for 1 h or more at 37°C. Activity of factor I was expressed as fluorescence of total free AMC released from FGR-AMC by the cleavage of factor I.

Coimmunoprecipitation

To examine the binding of factor I or factor H and Aβ, human purified factor I (210 ng) or human purified factor H (4.8 μg) and $A\beta_{1-40}$ (200 μM; final concentration) were added to 10 μM phosphate buffer (pH 7.4; containing 145 mM NaCl) to a final volume of 60 μl. After 1-h incubation at 37°C, the mixtures were reacted with 200 μl of factor I Ab or 200 μl of factor H Ab and further incubated at 4°C with gentle end-over-end mixing for 90 min. After incubation, 100 μl of 50% agarose slurry (protein G type) was added to both mixtures and further incubated at 4°C for 30 min with gentle end-over-end mixing. After 30 min of incubation, each mixture was centrifuged, the supernatant was removed, and the agarose containing factor I-Aβ complex or factor H-Aβ complex was washed with PBS three times before being loaded in diluted sample buffer (by PBS, 1/1) which did not contain DTT. The samples was heated for 5 min at 100°C and centrifuged. Then, 50 μl of the supernatant from each sample was respectively subjected to Western blot analysis using factor I Ab (MCA507, 1/200) or factor H Ab (MCA509, 1/200), and Aβ (4G8, 1/1000) Ab. Complex immunoreactivity was made visible by exposure of x-ray film to blots incubated with ECL reagent.

Statistical analyses

Data are expressed as means ± SEM. The significance level was set at $p < 0.05$. Statistical analysis was performed with the Mann-Whitney U test.

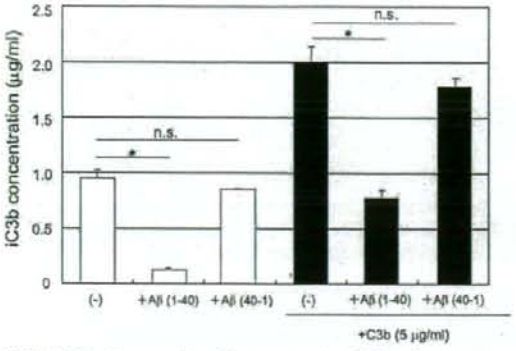

FIGURE 2. Concentration of immunoreactive iC3b in the supernatant of cultured RPE cells. Human RPE cells were incubated in the presence (50 μM) or absence of Aβ and/or C3b (5 μg/ml). The expression of iC3b protein in the culture supernatants was analyzed by ELISA after 24 h of culture. Values are expressed as the means ± SEMs. $n = 4$, *, $p < 0.05$.

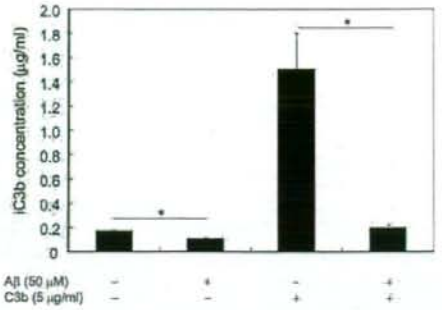

FIGURE 3. Decreased production of iC3b in the RPE cells in the presence of $A\beta_{1-40}$ using the transwell culture system. Cultured RPE cells were seeded into Costar cell culture inserts (0.4-μm pore size; Corning). Five days after cellular confluence, the medium was changed to serum-free DMEM. In this experiment, the exogenous C3b and $A\beta_{1-40}$ were added into the lower chamber. The conditioned media were also collected from the lower chamber, and the amount of iC3b was measured using ELISA. $n = 3$. *, $p < 0.05$.

Results

Expression of C3, C5, factor H, FHL, factor B, and factor I in RPE cells

The liver is the primary site of synthesis of the majority of the complement proteins in the human plasma. Extrahepatic biosynthesis of complement proteins may be an important factor in triggering and perpetuating local inflammatory reactions, especially in tissues that are shielded from the plasma components by a blood-tissue barrier. RT-PCR demonstrated the constitutive expression of the mRNAs for C3, C5, factor H, FHL, factor B, and factor I (Fig. 1) in the RPE cells. These findings suggest that RPE cells have a capacity to modulate the activation of the alternative pathway of complement.

C3b degradation is inhibited in Aβ-treated RPE cells

In all three pathways of complement activation, the pivotal step is the conversion of complement C3 to C3b, which is then covertly coupled to pathogens and Ag-Ab complexes. C3b is cleaved by factor I to iC3b in the presence of factor H and other cofactors (47). To determine whether C3b was cleaved by the RPE cells, we measured the level of iC3b in the supernatant by ELISA. Without exogenous C3b and $A\beta_{1-40}$, the average level of iC3b was 0.95 ± 0.08 μg/ml in the supernatants of RPE cells (Fig. 2). When the RPE cells were incubated with 50 μM $A\beta_{1-40}$ for 24 h, the amount of iC3b was significantly reduced to 0.13 ± 0.01 μg/ml ($p = 0.007$). When C3b (5 μg/ml) was added to the medium, the average amount of iC3b in the RPE cell supernatant was significantly increased to 2.00 ± 0.14 μg/ml. However, when 50 μM $A\beta_{1-40}$ was added to the medium, the amount of iC3b was significantly decreased to 0.78 ± 0.07 μg/ml ($p = 0.013$). In contrast, $A\beta_{40-1}$ alone had no effect on the cleavage of C3b.

When we added the $A\beta_{1-40}$ into the lower chamber using the transwell culture system, the amount of iC3b within the medium from the lower chamber was significantly decreased to 0.11 ± 0.01 μg/ml as compared with 0.175 ± 0.005 μg/ml within the medium from the nontreated RPE cells ($p = 0.034$) (Fig. 3). When C3b (5 μg/ml) was added into the lower medium, the average amount of iC3b was significantly increased to 1.5 ± 0.3 μg/ml. However, when 50 μM $A\beta_{1-40}$ was added to the lower medium together with C3b, the amount of iC3b was significantly decreased to 0.2 ± 0.02 μg/ml ($p = 0.0016$) (Fig. 3). In addition, the 50 μM $A\beta_{1-40}$ did not affect the cell viability as determined by the XTT assay (data not shown).

Addition of factor I restores iC3b production in Aβ-treated RPE cells

To confirm the direct contribution of either factor I or factor H in the decrease of C3b degradation by Aβ, we then examined the effect of purified factor I or factor H on Aβ-induced degradation of C3b. After changing the medium to serum-free medium, RPE cells were preincubated with (50 μM) or without $A\beta_{1-40}$ for 12 h. Then, 5 μg of rC3b was added to the medium, and the supernatant was collected after another 12 h. The amount of iC3b was determined by ELISA. The concentration of iC3b in the supernatants of nontreated RPE cells was 2.30 ± 0.10 μg/ml (Fig. 4), but the iC3b was significantly decreased to 0.87 ± 0.05 μg/ml in Aβ-treated RPE cells ($p = 0.013$). The addition of human purified factor I (1, 2, and 5 μg) significantly restored iC3b generation, but the addition of purified factor H (1, 2, and 5 μg) did not increase the amount of

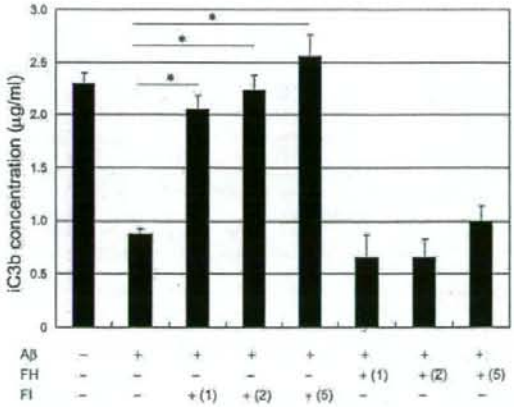

FIGURE 4. Effects of the addition of purified factor I or factor H on iC3b production in human RPE cells treated or not treated with Aβ. Twelve hours after changing the medium to serum-free DMEM supplemented with 50 μM Aβ and 5 μg/ml rC3b, purified factor H or factor I in different concentrations (1, 2, and 5 μg/ml) were added. After incubation for 12 more hours, the supernatants were collected and analyzed by ELISA for iC3b, $n = 3$. *, $p < 0.05$; FH, factor H; FI, factor I.

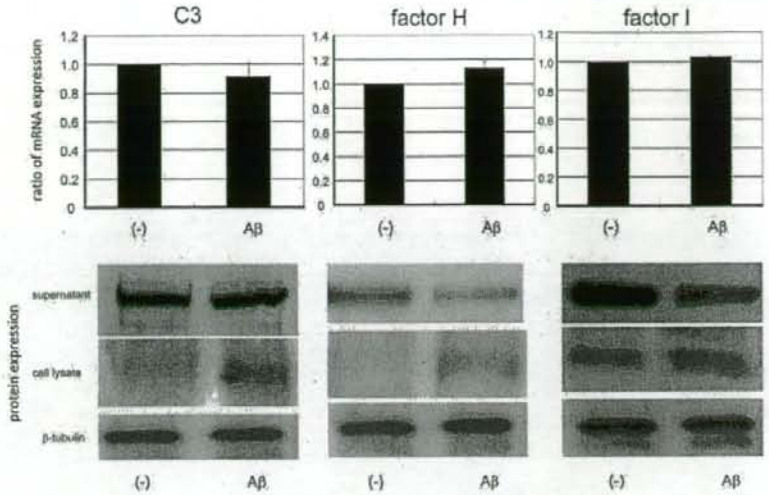

FIGURE 5. *Upper lane*, Real-time PCR analysis of cDNA of C3 (*left*), factor H (*center*), and factor I (*right*) prepared from RNA isolated from cultured human RPE cells in the presence or absence of Aβ (50 μM) for 24 h. The levels of mRNA are standardized to the level of GAPDH. The levels of mRNA of Aβ-treated RPE cells are shown as a ratio of those of nontreated RPE cells, and the averages of three samples (±SEMs) are plotted. Data are from five independent experiments. *Lower lane*, Immunoblot of C3 (*left*), factor H (*center*), and factor I (*right*) in cell lysates and the supernatants from human RPE cells in the presence or absence of 50 μM Aβ for 24 h. The supernatants (20 μl/lane) or cell lysates (80 μg/lane) were separated by SDS-PAGE, blotted onto nylon membrane, and detected with polyclonal anti-C3 (*left*), anti-factor H (*center*), or anti-factor I (*right*). This is a representative figure of five independent experiments.

iC3b, although the high concentration of factor H (5 μg) was able to restore iC3b generation in part.

Effects of Aβ on expression of gene and protein of C3, factor H, and factor I in human RPE cells

To determine whether the decrease of iC3b in the Aβ-treated RPE cells was due to a modified production of different complement-related proteins, we determined the expression of the mRNA and protein of C3, factor H, and factor I. The results showed that the expressions of the mRNA of C3, factor H, and factor I were not significantly different between RPE cells with and without Aβ treatment by real-time PCR ($p > 0.05$; Fig. 5, *upper lane*).

A representative photograph of a Western blot of C3, factor H, and factor I protein is shown in Fig. 5. Compared with nontreated RPE cells, the amount of C3 protein in the supernatants of Aβ-treated cells was similar, although it was slightly higher than that in the cell lysates. The secretion of factor H protein was decreased more in the supernatant of RPE cells treated with $Aβ_{1-40}$ than that in nontreated cells, and factor H protein was also increased in the Aβ-treated RPE cell lysates compared with nontreated cell lysates. The secretion of the protein of factor I was decreased more in the supernatant of Aβ-treated RPE cells than in nontreated cells; however, factor I protein was slightly increased in the cell lysates of Aβ-treated cells than in nontreated cell lysates.

Binding of Aβ with factor H and factor I

Because it has already been reported that Aβ binds to factor H (48), we investigated whether Aβ also forms a complex with factor I. Coimmunoprecipitation analysis detected a band in the 88-kDa area, which corresponded to the molecular mass of factor I, both

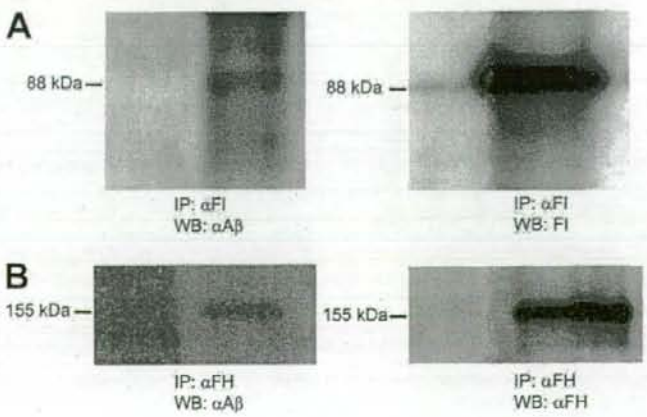

FIGURE 6. Coimmunoprecipitation of factor I-Aβ complex (*A*) and factor H-Aβ complex (*B*). Aβ and factor I or factor H were incubated in phosphate buffer (pH 7.4) for 1 h at 37°C before being loaded with factor I Ab or factor H Ab and further incubated at 4°C with gentle end-over-end mixing. Then, 50% agarose slurry (protein G type) was added to the mixture and further incubated at 4°C. Total mixture was centrifuged, supernatant was removed, and agarose-containing factor I-Aβ complex or factor H-Aβ complex was washed in PBS. The sample was centrifuged and the supernatant was subjected to Western blot analysis. The band in the 88-kDa area corresponding to factor I was detected by both factor I Ab (MCA507, 1/200) and Aβ Ab (4G8, 1/1000) (Fig. 5*A*). The band in the 155-kDa area corresponding to factor H was detected by both factor H Ab (MCA509, 1/200) and Aβ Ab (4G8, 1/1000) (Fig. 5*B*). FH, Factor H; FI, factor I; IP, immunoprecipitation; WB, Western blotting.

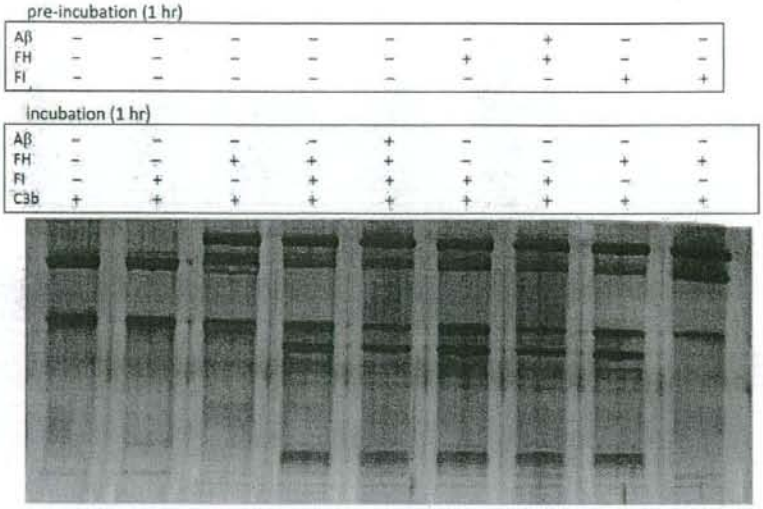

FIGURE 7. Preincubation of factor I with Aβ inhibits the cleavage of α-chain of C3b in a cofactor assay. Factor H and/or factor I were preincubated or not preincubated with Aβ (200 μM) for 1 h, and then mixed with C3b for another 1 h. All of the reactions were performed at 37°C in 10 μM phosphate buffer (pH 7.4) containing 145 mM NaCl and the reaction was stopped by the addition of SDS-PAGE buffer containing 2-ME. The reaction mixture was loaded onto 8% SDS-PAGE gel, and the cleavage products were made visible by silver staining. This is a representative photograph of five independent experiments. FH, Factor H; FI, factor I.

by Abs against factor I as well as against Aβ (Fig. 6*A*). Also, a band in the 155-kDa area, which corresponded to the molecular mass of factor H, was detected by the Abs against factor H and Aβ (Fig. 6*B*). These findings indicated that Aβ binds to factor I as well as factor H to form a complex.

Aβ affects activity of factor I but not factor H

We next analyzed whether Aβ affected the ability of factor I and factor H to cleave C3b. When C3b was incubated in only phosphate buffer, we detected two bands corresponding to the α- (110-kDa) and β- (70-kDa) chains of C3b (Fig. 7, *first lane*). The addition of factor H or factor I alone did not cause the degradation of C3b (Fig. 7, *second* and *third lanes*). When we incubated C3b with both factor H and factor I, two degradative fragments of the α-chain, viz., 68- and 43-kDa, appeared (Fig. 7, *fourth lane*). The absence of the 68- and 43-kDa fragments in reactions with C3b and factor I or factor H alone showed that both factor I and factor H are necessary for the cleavage of C3b under these conditions (Fig. 7, *fourth lane*). The presence of the 68- and 43-kDa fragments indicated that factor I mediated the cleavage of C3b between Arg^{1298} and Ser^{1299} in the generation of $iC3b_2$. Finally, when we simultaneously incubated C3b with factor H, factor I, and $A\beta_{1-40}$, the α-chain of C3b was also cleaved into two fragments (Fig. 7, *fifth lane*).

Next, we investigated whether preincubation of factor H or factor I with Aβ affected its ability to cleave of C3b. When factor H

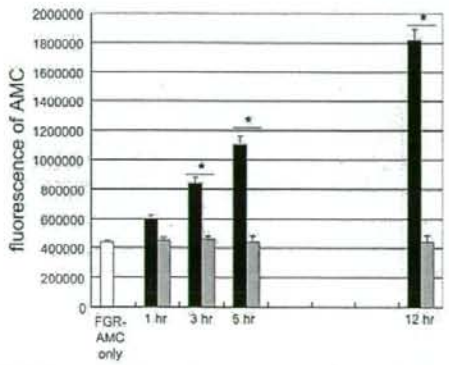

FIGURE 8. Amidolytic assay using synthetic substrate FGR-AMC. FGR-AMC (50 μM) and factor I (0.5 μM) in the presence (▨) or the absence (■) of 200 μM Aβ were incubated in 20 mM HEPES (pH 8.5) and at 37°C under light protection. Fluorescence of released AMC was measured by the excitation at 355 nm and emission at 460 nm, at different time points, $n = 3$; *, $p < 0.05$.

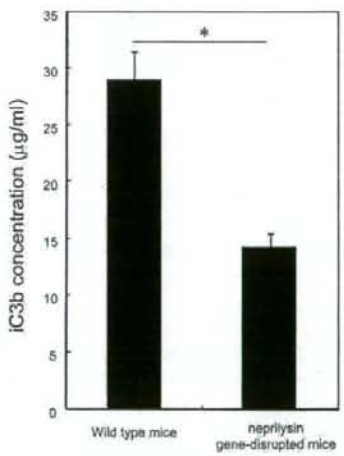

FIGURE 9. Decreased production of iC3b when C3b and factor H were incubated with the RPE-Bruch's membrane complex of neprilysin gene-disrupted mice as compared with that when C3b and factor H were incubated with the RPE-Bruch's membrane complex of wild-type mice. The RPE-Bruch's membrane-choriocapillaris complex was extracted from each four eyes of wild-type mice and neprilysin gene-disrupted mice. These complexes were then transferred into 40 μl of 10 μM phosphate buffer (pH 7.4; containing 145 mM NaCl) with C3b and factor H and incubated at 37°C for 12 h. After incubation, the supernatants were collected, diluted by 25 times in 10 μM phosphate buffer (pH 7.4, containing 145 mM NaCl), before being submitted to ELISA for iC3b. FH, Factor H; $n = 3$; *, $p < 0.05$.

was preincubated with $A\beta_{1-40}$ for 1 h, and then incubated with C3b and factor I for an additional 1 h, the degradation of the α-chain occurred (Fig. 7, *seventh lane*). However, when factor I was preincubated with $A\beta_{1-40}$ for 1 h before with C3b and factor H for another hour, the degradation of α-chain did not occur (Fig. 7, *ninth lane*). These results indicated that the preincubation with Aβ affected the ability of factor I, but not factor H, to cleave C3b into iC3b.

Effects of Aβ on the amidolytic activity of factor I

To further explore whether Aβ affected the function of factor I, we examined the amidolytic activity of factor I. This assay determines the levels of amidolytic activity of factor I against the FGR-AMC substrate without any cofactors. The addition of $A\beta_{1-40}$ abolished the amidolytic activity of factor I for 1–12 h (Fig. 8).

C3b degradative activity is decreased in the eyes of neprilysin gene-disrupted mice

Finally, we incubated the RPE-Bruch's membrane-choriocapillaris complex from the eyes of 12-mo-old neprilysin gene-disrupted mice or age-matched wild-type mice with exogenously added human C3b and factor H. The results demonstrated that the production of iC3b was significantly decreased to 14.2 ± 1.25 μg/ml when C3b and factor H were incubated with the eyes from neprilysin gene-disrupted mice compared with when C3b and factor H were incubated with the eyes from wild-type mice (29.0 ± 2.5 μg/ml; $p = 0.049$; Fig. 9).

Discussion

In our previous study regarding the developmental mechanism of AMD from drusen, (31) we focused on Aβ accumulated within drusen, and demonstrated that senescent neprilysin gene-disrupted mice which accumulate an excess amount of Aβ manifested similar features of human AMD. Although the mechanism for why Aβ induced the development of AMD was unclear, we hypothesized that Aβ-induced complement activation in subretinal tissue plays an important role for the development of AMD, and explored the mechanism of Aβ-induced complement activation in the present study.

Our results showed that the generation of inactivated C3b, and thus iC3b, was inhibited in RPE cells exposed to Aβ (Fig. 2). This finding was confirmed in experiments using the RPE-Bruch's membrane-choriocapillaris complex from neprilysin gene-disrupted mice (Fig. 9), which accumulated Aβ deposition in RPE cells as well as within the sub-RPE deposits, as we reported previously (31). The mechanism for this inhibition is the binding of Aβ to factor I which abolishes its ability to cleave its substrates as shown in two functional assays: the cofactor assay and the amidolytic assay.

Factor I is an 88-kDa serum glycoprotein which is a serine protease and cleaves the α-chains of C3b and C4b in the presence of its cofactor proteins (46). By inactivating C3b and C4b through limited proteolytic cleavage and thereby preventing the formation of the C3 and C5 convertases, factor I inhibits the alternative and the classical component pathways. Thus, the dysfunction of factor I accelerates the formation of the C3 convertase in the alternative pathway (45) resulting in unregulated complement activation.

Interestingly, the simultaneous incubation of Aβ with C3b, factor H, and factor I did not inhibit the C3b degradation in the cofactor assay. However, preincubation of factor I with Aβ abolished its ability to cleave the α-chain of C3b in the cofactor assay and to cleave FGR-AMC in the amidolytic assay. The HCl form of Aβ is known to be aggregated within 30 min when incubated in medium by The Peptide Institute (Osaka, Japan). This might suggest that the aggregation of Aβ might be necessary for the binding to factor I to Aβ as shown for the binding of factor H to Aβ (48). However, the mechanism of how the function of factor I is disturbed after binding to Aβ requires further investigation. As best we know, the binding of factor I to Aβ has not been reported, while the binding of factor H to the aggregated fibrillar form of Aβ has been reported (48). Aggregated fibrillar Aβ is generally considered to be a rather sticky complex capable of binding proteins nonspecifically, although a charge-based interaction might be one possibility as suggested by Strohmeyer and associates (48).

Western blot analyses showed that exposure of RPE cells to Aβ decreased the amount of factor H and factor I secreted into the supernatant of cultured RPE cells (Fig. 5), while Western blot analyses using cell lysates showed that the amount of C3, factor H, and factor I was increased in Aβ-treated RPE cells (Fig. 5). This difference might be because Aβ binds to these molecules and traps them possibly on the cell membrane as reported (43). Thus, not only the dysfunction of factor I by binding to Aβ, but also a decrease of the secreted amount of free factor H and factor I into the subretinal space might be involved in the process of the unregulated activation of complement.

The extrahepatic biosynthesis of complement is considered to be an important source of complement which triggers and perpetuates local inflammatory reactions, especially in tissues that are shielded from the plasma components by a blood-tissue barrier such as the retina. By using specific primers and RT-PCR, we demonstrated that human RPE cells constitutively express the major components of the complement alternative pathway, including C3, factor B, factor H, FHL, C5, and factor I (Figs. 1 and 2). A Medline search identified only one publication that reported the synthesis of factor H by human and mouse RPE cells (49). However, we did not find any publications for the expression of the other complement components by RPE cells.

The expression of various complement components in human RPE cells suggests that most of the complement proteins and their regulators that are present within the drusen and in the subretinal space can be synthesized by RPE cells, although some of the proteins may be derived from the choroidal circulation. Therefore, it is highly likely that the RPE cells regulate the activation of the complement pathway and maintain this aspect of retinal homeostasis under physiological conditions. However, once the RPE cells become senescent or pathological, the regulation of the complement pathway might be disturbed.

Although recent genetic studies suggested an important role of the complement system for the pathogenesis of AMD (12–17, 20–23), we suspect that this is probably due to the tissue specificity of the macular area in the eye. The retina is shielded from the plasma components by a blood-tissue barrier like the brain, and furthermore, the retina of the macular area is completely avascular. In such kind of shielded tissue, once unregulated complement activation induced by the accumulated Aβ occurs, it might be difficult to stop the amplification loop. Subsequently, the chronic exposure of RPE cells to bioactive fragments of complement components might induce pathological damage on RPE cells. In addition, chronic activation of complement might cause a migration of monocytes that might be involved in the degradation of Bruch's membrane.

Chronic inflammation induced by complement activation is also considered to be a significant contributor to the neurodegenerative processes in the brains of patients with AD (35, 36, 43, 50, 51). In any case, the pathogenesis of AD and AMD may have many similarities, and the observations made in our study might also apply to the brain of AD patients.

For AMD to develop, an interaction between the environment and genetic susceptibility has been considered to be critical. Very recently, Campochiaro and colleagues demonstrated that oxidative stress reduces the ability of IFN-γ, an inflammatory cytokine, to increase the expression of factor H in RPE cells (52). Also, in an investigation of a potential trigger for complement activation in AMD, Zhou et al. (53) explored the idea that the complex mixture of products resulting from photo-oxidation of A2E might include a range of fragments that could be recognized by the complement system as "foreign," and could activate the complement system, leading to low-grade inflammation. A2E is a bis-retinoid pigment which accumulates as lipofuscin in RPE. They found that iC3b and C3a were elevated in the medium overlying ARPE-19 cells that had accumulated A2E and were irradiated to induce A2E photo-oxidation. In our study, we showed that Aβ directly inactivated factor I. Taken together (52, 53), these data suggest that there are important interactions between environmental exposures and genetic susceptibilities in the pathogenesis of AMD.

In conclusion, we have demonstrated that Aβ binds to factor I and blocks its ability to inhibit the inactivation of C3b, resulting in unregulated complement activation. Our findings provide new insights into the pathogenesis and the treatment strategies of AMD, especially to prevent the progression to AMD from its earliest clinical hallmark of drusen deposits.

Acknowledgments

We thank Prof. Duco Hamasaki for critical discussion and revision of the final manuscript. We also thank Prof. Peter A. Campochiaro and Sean F. Hackett for human RPE cells. We thank M. Sekiguchi, K. Watanabe, and R. Fujioka (RIKEN Brain Institute) for technical assistance.

Disclosures

The authors have no financial conflict of interest.

References

1. Gasque, P. 2004. Complement: a unique innate immune sensor for danger signals. *Mol. Immunol.* 41: 1089–1098.
2. Mayer, M. 1973. The complement system. *Sci. Am.* 229: 54–66.
3. Barnum, S. 1995. Complement biosynthesis in the central nervous system. *Crit. Rev. Oral Biol. Med.* 6: 132–146.
4. Sommer, A., J. M. Tielsch, J. Katz, H. A. Quigley, J. D. Gottsch, J. C. Javitt, J. F. Martone, R. M. Royall, K. A. Witt, and S. Ezrine. 1991. Racial differences in the cause-specific prevalence of blindness in east Baltimore. *N. Engl. J. Med.* 325: 1412–1417.
5. Attebo, K., P. Mitchell, and W. Smith. 1996. Visual acuity and the causes of visual loss in Australia. The Blue Mountains Eye Study. *Ophthalmology* 103: 357–364.
6. VanNewkirk, M. R., L. Weih, C. A. McCrty, and H. R. Taylor. 2001. Cause-specific prevalence of bilateral impairment in Victoria, Australia: the Visual Impairment Project. *Ophthalmology* 108: 960–967.
7. Oshima, Y., T. Ishibashi, T. Murata, Y. Tahara, Y. Kiyohara, and T. Kubota. 2001. Prevalence of age-related maculopathy in a representative Japanese population: the Hisayama study. *Br. J. Ophthalmol.* 85: 1153–1157.
8. Johnson, L. V., W. P. Leitner, M. K. Staples, and D. H. Anderson. 2001. Complement activation and inflammatory processes in drusen formation and age related macular degeneration. *Exp. Eye Res.* 73: 887–896.
9. Ambati, J., A. Anand, S. Fernandez, E. Sakurai, B. C. Lynn, W. A. Kuziel, B. J. Rollins, and B. K. Ambati. 2003. An animal model of age-related macular degeneration in senescent Ccl-2- or Ccr-2-deficient mice. *Nat. Med.* 9: 1390–1397.
10. Hageman, G. S., P. J. Luthert, N. H. V. Chong, L. V. Johnson, D. H. Anderson, and R. F. Mullins. 2001. An integrated hypothesis that considers drusen as biomarkers of immune-mediated processes at the RPE-Bruch's membrane interface in aging and age-related macular degeneration. *Prog. Retin. Eye Res.* 20: 705–732.
11. Nozaki, M., B. J. Raisler, E. Sakurai, J. V. Sarma, S. R. Barnum, J. D. Lambris, Y. Chen, K. Zhang, B. K. Ambati, J. Z. Baffi, and J. Ambati. 2006. Drusen complement components C3a and C5a promote choroidal neovascularization. *Proc. Natl. Acad. Sci. USA* 103: 2328–2333.
12. Klein, R. J., C. Zeiss, E. Y. Chew, J. Y. Tsai, R. S. Sackler, C. Haynes, A. K. Henning, J. P. SanGiovanni, S. M. Mane, S. T. Mayne, et al. 2005. Complement factor H polymorphism in age-related macular degeneration. *Science* 308: 385–389.
13. Edwards, A. O., R. Ritter, K. J. Abel, A. Manning, C. Panhuysen, and L. A. Farrer. 2005. Complement factor H polymorphism and age-related macular degeneration. *Science* 308: 421–424.
14. Haines, J. L., M. A. Hauser, S. Schmidt, W. K. Scott, L. M. Olson, P. Gallins, K. L. Spencer, S. Y. Kwan, M. Noureddine, J. R. Gilbert, et al. 2005. Complement factor H variant increases the risk of age-related macular degeneration. *Science* 308: 419–421.
15. Hageman, G. S., D. H. Anderson, L. V. Johnson, L. S. Hancox, A. J. Taiber, L. I. Hardisty, J. L. Hageman, H. A. Stockman, J. D. Borchardt, K. M. Gehrs, et al. 2005. A common haplotype in the complement regulatory gene factor H (HF1/CFH) predisposes individuals to age-related macular degeneration. *Proc. Natl. Acad. Sci. USA* 102: 7227–7232.
16. Gold, B., J. B. Merriam, J. Zernant, L. S. Hancox, A. J. Taiber, K. Gehrs, K. Cramer, J. Neel, J. Bergeron, G. R. Barile, et al. 2006. Variation in factor B (BF) and complement component 2 (C2) genes is associated with age-related macular degeneration. *Nat. Genet.* 38: 458–462.
17. Maller, J., S. George, S. Purcell, J. Fagerness, D. Altshuler, M. J. Daly, and J. M. Seddon. 2006. Common variation in three genes, including a noncoding variant in CFH, strongly influences risk of age-related macular degeneration. *Nat. Genet.* 38: 1055–1059.
18. Whaley, K., and S. Ruddy. 1976. Modulation of the alternative complement pathways by β1 H globulin. *J. Exp. Med.* 144: 1147–1163.
19. Weiler, J. M., M. R. Daha, K. F. Austen, and D. T. Fearon. 1976. Control of the amplification convertase of complement by the plasma protein β1 H. *Proc. Natl. Acad. Sci. USA* 73: 3268–3272.
20. Jakobadottir, J., Y. P. Conley, D. E. Weeks, T. S. Mah, R. E. Ferrell, and M. B. Gorin. 2005. Susceptibility genes for age-related maculopathy on chromosome 10q26. *Am. J. Hum. Genet.* 77: 389–407.
21. Dewan, A., M. Liu, S. Hartman, S. S. Zhang, D. T. Liu, C. Zhao, P. O. Tam, W. M. Chan, D. S. Lam, M. Snyder, et al. 2006. HTRA1 promoter polymorphism in wet age-related macular degeneration. *Science* 314: 989–992.
22. Yang, Z., N. J. Camp, H. Sun, Z. Tong, D. Gibbs, D. J. Cameron, H. Chen, Y. Zhao, E. Pearson, X. Li, et al. 2006. A variant of the *HTRA1* gene increases susceptibility of age-related macular degeneration. *Science* 314: 992–993.
23. Yates, J. R. W., T. Sepp, B. K. Matharu, J. C. Khan, D. A. Thurlby, H. Shahid, D. G. Clayton, C. Hayward, J. Morgan, A. F. Wright, et al. 2007. Complement C3 variant and the risk of age-related macular degeneration. *N. Engl. J. Med.* 357: 19–27.
24. Mullins, R. F., S. R. Russell, D. H. Anderson, and G. S. Hageman. 2000. Drusen associated with aging and age-related macular degeneration contain proteins common to extracellular deposits associated with atherosclerosis, elastosis, amyloidosis, and dense deposit disease. *FASEB J.* 14: 835–846.
25. Bora, N. S., S. Kaliappan, P. Jha, Q. Xu, J. H. Sohn, D. B. Dhaulakhandi, H. J. Kaplan, and P. S. Bora. 2006. Complement activation via alternative pathway is critical in the development of laser-induced choroidal neovascularization: role of factor B and factor H. *J. Immunol.* 117: 1872–1878.
26. Green, R. G., and J. B. Harlan. 1999. Histopathologic features. In *Age-Related Macular Degeneration.* J. W. Berger, S. L. Fine, and M. G. Maguire, eds. Mosby, St. Louis, pp. 81–154.
27. Bressler, S. B., M. G. Maguire, N. M. Bressler, and S. L. Fione. 1990. Relationship of drusen and abnormalities of the retinal pigment epithelium to the prognosis of neovascular macular degeneration. The Macular Photocoagulation Study Group. *Arch. Ophthalmol.* 108: 1442–1447.
28. Mukesh, B. N., P. N. Dimitrov, S. Leikin, J. J. Wang, P. Mitchel, C. A. McCarty, and H. R. Taylor. 2004. Five-year incidence of age-related maculopathy: the Visual Impairment Project. *Ophthalmology* 111: 1176–1182.
29. Johnson, L. V., W. P. Leitner, A. J. Rivest, M. K. Staples, M. J. Radeke, and D. H. Anderson. 2002. The Alzheimer's Aβ-peptide is deposited at sites of complement activation in pathologic deposits associated with aging and age-related macular degeneration. *Proc. Natl. Acad. Sci. USA* 99: 11830–11835.
30. Crabb, J. W., M. Miyagi, X. Gu, K. Shadrach, K. A. West, H. Sakaguchi, M. Kamei, A. Hasan, L. Yan, M. E. Rayborn, et al. 2002. Drusen proteome analysis: an approach to the etiology of age-related macular degeneration. *Proc. Natl. Acad. Sci. USA* 99: 14682–14687.
31. Yoshida, T., K. Ohno-Matsui, S. Ichinose, T. Sato, N. Iwata, T. C. Saido, T. Hisatomi, M. Mochizuki, and I. Morita. 2005. The potential role of amyloid β in the pathogenesis of age-related macular degeneration. *J. Clin. Invest.* 115: 2793–2800.
32. Vassar, R., B. D. Bennet, S. Babu-Khan, S. Kahn, E. A. Mendiaz, P. Denis, D. B. Teplow, S. Ross, P. Amarante, R. Loeloff, et al. 1999. β-secretase cleavage of Alzheimer's amyloid precursor protein by the transmembrane aspartic protease BACE. *Science* 286: 735–741.
33. Takasugi, N., T. Tomita, I. Hayashi, M. Tsuruoka, M. Niimura, Y. Takahashi, G. Thinakaran, and T. Iwatsubo. 2003. The role of presenilin cofactors in the γ-secretase complex. *Nature* 422: 438–441.
34. Haass, C., and D. J. Selkoe. 2007. Soluble protein oligomers in neurodegeneration: lessons from the Alzheimer's amyloid-β peptide. *Nat. Mol. Cell Biol.* 8: 101–112.
35. Akiyama, S., S. Barger, S. Barnum, B. Bradt, J. Bauer, G. M. Cole, N. R. Cooper, P. Eikelenboom, M. Emmerling, B. L. Fiebich, et al. 2000. Inflammation and Alzheimer's disease. *Neurobiol. Aging* 21: 383–421.
36. Bradt, B. M., W. P. Kolb, and N. R. Cooper. 1998. Complement-dependent proinflammatory properties of the Alzheimer's disease β-peptide. *J. Exp. Med.* 188: 431–438.
37. Ohno-Matsui, K., I. Morita, J. Tombran-Tink, D. Mrazek, M. Onoders, T. Uetama, M. Hayano, S. I. Murota, and M. Mochizuki. 2001. Novel mechanism

for age-related macular degeneration: an equilibrium shift between the angiogenesis factors VEGF and PEDF. *J. Cell. Physiol.* 189: 323–333.
38. Campochiaro, P. A., and S. F. Hackett. 1993. Corneal endothelial cell matrix promotes expression of differentiated features of retinal pigment epithelial cells: implication of laminin and basic fibroblast growth factor as active components. *Exp. Eye Res.* 57: 539–547.
39. Hellwage, J., S. Kuhn, and P. F. Zipfel. 1997. The human complement regulatory factor-H-like protein 1, which represents a truncated form of factor H, displays cell-attachment activity. *Biochem. J.* 326: 321–327.
40. Klegris, A., C. J. Bissonnette, K. Dorovini-Zis, and P. L. McGeer. 2000. Expression of complement messenger RNAs by human endothelial cells. *Brain Res.* 871: 1–6.
41. Friese, M. A., T. Manuelian, S. Junnikkala, J. Hellwage, S. Meri, H. H. Peter, D. L. Gordon, H. Eibel, and P. F. Zipfel. 2003. Release of endogenous anti-inflammatory complement regulators FHL-1 and factor H protects synovial fibroblasts during rheumatoid arthritis. *Clin. Exp. Immunol.* 132: 485–495.
42. Pasch, M. C., N. H. A. van den Bosch, M. R. Daha, J. D. Bos, and S. S. Asghar. 2000. Synthesis of complement components C3 and factor B in human keratinocytes is differentially regulated by cytokines. *J. Invest. Dermatol.* 114: 78–82.
43. Strohmeyer, R., Y. Shen, and J. Rogers. 2000. Detection of complement alternative pathway mRNA and proteins in the Alzheimer's disease brain. *Mol. Brain Res.* 81: 7–18.
44. Kai, S., T. Fujita, I. Gigli, and V. Nussenzweig. 1980. Mouse C3b/C4b inactivator: purification and properties. *J. Immunol.* 125: 2409–2415.
45. Sahu, A., S. N. Isaacs, A. M. Soulika, and J. D. Lambris. 1998. Interaction of vaccinia virus complement control protein with human complement proteins: factor I-mediated degradation of C3b to iC3b$_1$ inactivates the alternative complement pathway. *J. Immunol.* 160: 5596–5604.
46. Tsiftsoglou, S. A., A. C. Willis, P. Li, X. Chen, D. A. Mitchell, Z. Rao, and R. B. Sim. 2005. The catalytically active serine protease domain of human complement factor I. *Biochemistry* 44: 6239–6249.
47. Nilsson, B., and K. N. Ekdahl. 1998. Components of the alternative pathway. In *The Complement System.* K. Rother, G. O. Till, and G. M. Hansch, eds. Springer, New York, pp. 23–49.
48. Strohmeyer, R., M. Ramirez, G. J. Cole, K. Mueller, and J. Rogers. 2002. Association of factor H of the alternative pathway of complement with agrin and complement receptor 3 in the Alzheimer's disease brain. *J. Neuroimmunol.* 131: 135–146.
49. Chen, M., V. John, and H. Xu. 2006. Synthesis of complement factor H by retinal pigment epithelial cells is down-regulated by oxidized photoreceptor outer segments. *Exp. Eye Res.* 84: 635–645.
50. Rogers, J., N. R. Cooper, S. Webster, J. Schultz, P. L. McGeer, S. D. Styren, W. H. Civin, L. Brachova, B. Bradt, P. Ward, and I. Lieberburg. 1992. Complement activation by β-amyloid in Alzheimer disease. *Proc. Natl. Acad. Sci. USA* 89: 10016–10020.
51. Webster, S., L. F. Lue, L. Brachova, A. J. Tenner, P. L. McGeer, K. Terai, D. G. Walker, B. Bradt, N. R. Cooper, and J. Rogers. 1997. Molecular and cellular characterization of the membrane attack complex, C5b-9, in Alzheimer's disease. *Neurobiol. Aging* 18: 415–421.
52. Wu, Z., T. W. Lauer, A. Sick, S. F. Hackett, and P. A. Campochiaro. 2007. Oxidative stress modulates complement factor H expression in retinal pigmented epithelial cells by acetylation of FOXO3. *J. Biol. Chem.* 282: 22414–22425.
53. Zhou, L., Y. P. Jang, S. R. Kim, and J. R. Sparrow. 2006. Complement activation by photooxidation products of A2E, a lipofuscin constituent of the retinal pigment epithelium. *Proc. Natl. Acad. Sci. USA* 103: 16182–16187.

THE JOURNAL OF BIOLOGICAL CHEMISTRY VOL. 283, NO. 28, pp. 19489–19498, July 11, 2008

Evidence That CD147 Modulation of β-Amyloid (Aβ) Levels Is Mediated by Extracellular Degradation of Secreted Aβ*◆

Received for publication, February 7, 2008, and in revised form, April 30, 2008 Published, JBC Papers in Press, May 1, 2008, DOI 10.1074/jbc.M801037200

Kulandaivelu S. Vetrivel[‡1], Xulun Zhang[‡1], Xavier Meckler[‡], Haipeng Cheng[‡], Sungho Lee[‡], Ping Gong[‡], Kryslaine O. Lopes[‡], Ying Chen[‡], Nobuhisa Iwata[§], Ke-Jie Yin[¶], Jin-Moo Lee[¶], Angèle T. Parent[‡], Takaomi C. Saido[§], Yue-Ming Li[‖], Sangram S. Sisodia[‡2], and Gopal Thinakaran[‡3]

From the [‡]Departments of Neurobiology and Neurology, The University of Chicago, Chicago, Illinois 60637, the [§]Laboratory for Proteolytic Neuroscience, RIKEN Brain Science Institute, 2-1 Hirosawa, Wako-shi, Saitama 351-0198, Japan, the [¶]Department of Neurology and the Hope Center for Neurological Disorders, Washington University School of Medicine, St. Louis, Missouri 63110, and the [‖]Molecular Pharmacology and Chemistry Program, Memorial Sloan-Kettering Cancer Center, New York, New York 10021

Cerebral deposition of β-amyloid (Aβ) peptides is a pathological hallmark of Alzheimer disease. Intramembranous proteolysis of amyloid precursor protein by a multiprotein γ-secretase complex generates Aβ. Previously, it was reported that CD147, a glycoprotein that stimulates production of matrix metalloproteinases (MMPs), is a subunit of γ-secretase and that the levels of secreted Aβ inversely correlate with CD147 expression. Here, we show that the levels and localization of CD147 in fibroblasts, as well as postnatal expression and distribution in brain, are distinct from those of integral γ-secretase subunits. Notably, we show that although depletion of CD147 increased extracellular Aβ levels in intact cells, membranes isolated from CD147-depleted cells failed to elevate Aβ production in an *in vitro* γ-secretase assay. Consistent with an extracellular source that modulates Aβ metabolism, synthetic Aβ was degraded more rapidly in the conditioned medium of cells overexpressing CD147. Moreover, modulation of CD147 expression had no effect on ε-site cleavage of amyloid precursor protein and Notch1 receptor. Collectively, our results demonstrate that CD147 modulates Aβ levels not by regulating γ-secretase activity, but by stimulating extracellular degradation of Aβ. In view of the known function of CD147 in MMP production, we postulate that CD147 expression influences Aβ levels by an indirect mechanism involving MMPs that can degrade extracellular Aβ.

Alzheimer disease is an age-associated neurodegenerative disorder that is clinically manifested by the progressive loss of memory and cognitive functions. An early event in the development of Alzheimer disease is the aggregation and deposition of β-amyloid (Aβ)[4] peptides in the brains of affected individuals. Aβ is derived from type I transmembrane protein, termed amyloid precursor protein (APP), through sequential cleavage by β- and γ-secretases (1, 2). γ-Secretase is a multimeric protein complex consisting of presenilin (PS1 or PS2), nicastrin, APH1, and PEN-2 as core subunits (2). The exact functional contribution of each γ-secretase subunit to enzyme activity has not been fully elucidated, but multiple lines of evidence suggest that PS1, a protein that accumulates as endoproteolytically processed N-terminal (NTF) and C-terminal (CTF) fragments, is the catalytic center of γ-secretase, whereas nicastrin appears to facilitate substrate recruitment (3–5). Coexpression of these four transmembrane proteins is sufficient to reconstitute γ-secretase activity in yeast, an organism that lacks orthologous proteins (6). Gene knock-out and small interfering RNA (siRNA)-mediated knockdown studies have demonstrated that Aβ production is compromised in the absence of any one of these core components (7–10). Collectively, these latter studies establish that PS1, nicastrin, APH1, and PEN-2 are necessary and sufficient for γ-secretase processing of APP.

The biogenesis, maturation, stability, and steady-state levels of γ-secretase complex subunits are codependent (reviewed in Ref. 11). For example, limiting expression of any one of the integral components affects the post-translational maturation and stability of the other subunits, indicating that their assembly into high molecular mass complexes is a highly regulated process that occurs during biosynthesis of these polypeptides. In this regard, the heavily glycosylated type I membrane protein nicastrin does not mature and exit the endoplasmic reticulum (ER) in cells lacking PS1 expression (12). On the other hand, PS1 fails to undergo endoproteolysis to generate stable NTFs

* This work was supported, in whole or in part, by National Institutes of Health Grants AG021495 and AG019070 (to G. T.) and AG026660 (to Y.-M. L.). This work was also supported by Grants-in-aid for Scientific Research on Priority Areas 17025046 and 18023037 from the Ministry of Education, Culture, Sports, Science, and Technology of Japan (to N. I.), by an Alzheimer's Association Investigator-Initiated research grant (to G. T.) and new investigator research grant (to K. S. V.), and by grants from the American Health Assistance Foundation (to G. T. and S. S. S.). The costs of publication of this article were defrayed in part by the payment of page charges. This article must therefore be hereby marked "*advertisement*" in accordance with 18 U.S.C. Section 1734 solely to indicate this fact.

◆ This article was selected as a Paper of the Week.

[1] Both authors contributed equally to this work.

[2] To whom correspondence may be addressed: Dept. of Neurobiology, The University of Chicago, Abbott 308, 947 E. 58th Street, Chicago, IL 60637. Tel.: 773-834-9186; Fax: 773-702-2926; E-mail: ssisodia@bsd.uchicago.edu.

[3] To whom correspondence may be addressed: Dept. of Neurobiology, The University of Chicago, Knapp R212, 924 E. 57th St., Chicago, IL 60637. Tel.: 773-834-3752; Fax: 773-834-3808; E-mail: gopal@uchicago.edu.

[4] The abbreviations used are: Aβ, β-amyloid; APP, amyloid precursor protein; PS, presenilin; NTF, N-terminal fragment; CTF, C-terminal fragment; siRNA, small interfering RNA; ER, endoplasmic reticulum; MMP, matrix metalloproteinase; MEFs, mouse embryonic fibroblasts; CHAPSO, 3-[(3-cholamidopropyl)dimethylammonio]-2-hydroxy-1-propanesulfonic acid; DRM, detergent-resistant membrane; MOPS, 4-morpholinepropanesulfonic acid; ELISA, enzyme-linked immunosorbent assay; WT, wild-type; AICD, APP intracellular domain; NICD, Notch intracellular domain; Tricine, *N*-[2-hydroxy-1,1-bis(hydroxymethyl)ethyl]glycine.

and CTFs in cells lacking nicastrin, APH1a, or PEN-2 expression (11). The use of detergents with dissimilar solubilization properties and different biochemical purification methods has led to discrepant size predictions of the active γ-secretase complexes, with estimates ranging from 250 kDa to 2 MDa (13, 14). Although a recent study has shown that active γ-secretase contains one of each of these four essential components (15), it is notable that the estimated sizes of the γ-secretase complexes exceed the sum of the four integral subunits. Thus, it is generally anticipated that one or more cofactors might associate with the four integral subunits of the γ-secretase complex and that these polypeptides modulate enzyme activity.

Recently, two type I membrane proteins, CD147 and p23, have been shown to co-immunoisolate with the γ-secretase complex and regulate Aβ levels (16, 17). CD147 (also called EMMPRIN (extracellular matrix metalloproteinase inducer), Basigin, neurothelin, and M6 leukocyte activation antigen) is a multifunctional cell-surface type I transmembrane protein that stimulates matrix metalloproteinase (MMP) secretion (18). p23 (also called TMP21) is a member of the p24 type I transmembrane protein family involved in vesicular trafficking between the ER and Golgi (19). siRNA-mediated knockdown of CD147 or p23 expression causes dose-dependent increases in the levels of secreted Aβ (16, 17). Nevertheless, because only a small fraction of the cellular pool of CD147 or p23 remains complexed with γ-secretase at steady state, the precise mechanisms by which these proteins modulate γ-secretase activity remain obscure. For example, p23 influences Aβ levels by modulating γ-secretase cleavage of APP and by regulating secretory trafficking of APP and possibly APP secretases (20). In this study, we show that CD147 does not directly modulate γ-secretase cleavage of APP substrate in an *in vitro* γ-secretase assay. Instead, we found evidence for enhanced degradation of Aβ in medium conditioned by cells overexpressing CD147, suggesting the potential involvement of CD147-induced MMP secreted forms in modulating extracellular Aβ levels. Consistent with this indirect mechanism, the absence of PS1 and nicastrin has no effect on CD147 stability and subcellular localization, and CD147 expression fails to influence γ-secretase subunit expression and lipid raft association. A distinct expression pattern and distribution of CD147 and nicastrin in brain further support our view that CD147 regulates extracellular Aβ levels via mechanisms independent of γ-secretase processing of APP.

EXPERIMENTAL PROCEDURES

cDNA Constructs and Oligonucleotides—Human CD147 cDNA was generated by reverse transcription-PCR using total RNA isolated from HEK293 cells. C-terminally Myc/His-tagged CD147 was constructed by subcloning CD147 cDNA into the pAG3-Myc-His vector. The following primers were used to generate RNA duplexes using a Silencer siRNA construction kit (Ambion): CD147 siRNA, AAGACCTTGGCTCCAAGATACCCTGTCTC and AAGTATCTTGGAGCCAAGGTCCCTGTCTC; and scrambled siRNA, AACTCTTCCGCGTAGCAAAGACCTGTCTC and AATCTTTGCTACGCGGAAGAGCCTGTCTC. The cDNA encoding C-terminally Myc-tagged APP (APPswe-6Myc) (a kind gift from Dr. Alison Goate) (21) was subcloned into the pCB6 vector. An expression plasmid encoding truncated Notch1 (mNotchΔE) was kindly provided by Dr. Jeffrey S. Nye.

Cell Lines—Mouse embryonic fibroblasts (MEFs) and HEK293 cells were maintained in Dulbecco's modified Eagle's medium supplemented with 10% fetal bovine serum. HEKswe cells were maintained in the presence of 200 μg/ml G418 (22). HEK293 cells were transfected with CD147-Myc-His plasmid, and stable transfectants were selected as pools in the presence of 200 μg/ml Zeocin. $PS1^{-/-}/PS2^{-/-}$ and $NCT^{-/-}$ cells stably expressing PS1 or nicastrin were generated by retroviral infections of MEFs and selected in the presence of 4 μg/ml puromycin as described previously (23). CD147 and scrambled siRNA duplexes were transfected into HEK293 cells using Lipofectamine (Invitrogen) and analyzed after 48 h.

Co-immunoprecipitation—$PS1^{-/-}/PS2^{-/-}$ cells stably expressing either vector or PS1 were lysed in buffer containing 1% CHAPSO, 25 mM HEPES (pH 7.4), 150 mM NaCl, 2 mM EDTA, and a mixture of protease inhibitors. Equal amounts of proteins from the post-nuclear supernatants were used for co-immunoisolation using the $PS1_{NT}$ antibody as described previously (24).

Protein Analysis, Immunostaining, and Detergent-resistant Membrane (DRM) Isolation—Total protein lysates from cultured cells and mouse brain harvested during embryonic and postnatal developmental stages were prepared essentially as described previously (25). Antibodies against γ-secretase subunits, APP, and organelle markers have been described (26). Goat anti-CD147 (Santa Cruz Biotechnology) and anti-human CD147 (Chemicon) monoclonal antibodies were used to detect CD147. Immunofluorescence staining and isolation of DRMs from Lubrol WX lysates of cultured cells by discontinuous flotation density gradients were performed as described (26, 27). Immunohistochemical staining was performed on 30-μm sagittal sections of 2-month-old C57BL/6J mouse brain with rabbit anti-nicastrin (SP718; 1:1000) or goat anti-CD147 (1:5000) antibody as described (28).

In Vitro γ-Secretase Assays—Membranes prepared from HEK293 cells transfected with either scrambled or CD147 siRNA were used to examine γ-secretase activity using C100-FLAG substrate as described previously (14). Briefly, cells were homogenized 10 times using a glass-Teflon homogenizer in buffer containing 10 mM MOPS, 10 mM KCl, 1 mM EDTA, and protease inhibitor mixture. The homogenate was subjected to centrifugation at 1000 × *g* for 10 min at 4 °C. The supernatant was saved, and the pellet was passed through one more round of homogenization. Pooled supernatants were centrifuged at 100,000 × *g* for 1 h at 4 °C. The resulting pellet was resuspended in homogenization buffer and centrifuged again at 100,000 × *g* for 1 h at 4 °C. The pellet-containing membranes were used for *in vitro* γ-secretase activity assay in the presence or absence of 1 μM L685,458 to establish the specificity of the assay.

Aβ Digestion Assay Using Synthetic Aβ—9 μl of culture medium was incubated with 6 ng of synthetic $Aβ_{40}$ or $Aβ_{42}$ for 14 h at 37 °C. After incubation, the reaction mixtures were resolved by gradient SDS-PAGE followed by Western blotting using monoclonal antibody 6E10.

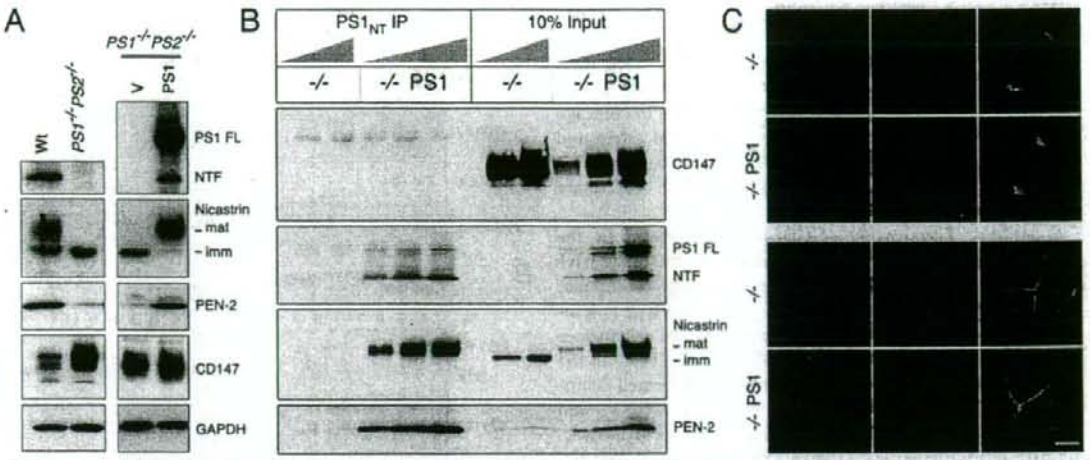

FIGURE 1. **Subcellular localization of CD147 in the absence of γ-secretase subunit expression.** *A*, comparison of the steady-state levels of CD147 and γ-secretase subunits. Total cell lysates from WT and $PS1^{-/-}/PS2^{-/-}$ MEFs and $PS1^{-/-}/PS2^{-/-}$ pools stably transduced with retrovirus harboring empty vector or human PS1 cDNA were probed with the indicated antibodies. Similar results were obtained in two independent pools of stably transduced cells. *FL*, full-length; *mat*, mature; *imm*, immature; *GAPDH*, glyceraldehyde-3-phosphate dehydrogenase. *B*, co-immunoprecipitation analysis of CD147 with γ-secretase subunits. $PS1^{-/-}/PS2^{-/-}$ MEFs stably overexpressing empty vector or human PS1 were lysed in 1% CHAPSO, co-immunoprecipitated using the $PS1_{NT}$ antibody as described under "Experimental Procedures," and probed with the indicated antibodies. Note that the endogenous γ-secretase components nicastrin and PEN-2 co-immunoprecipitated with PS1; CD147 was not detected as part of the immunoprecipitated complex. Similar results were obtained in co-immunoprecipitation analysis of mouse N2a neuroblastoma cells and HEK293 cells. *C*, analysis of the indicated $PS1^{-/-}/PS2^{-/-}$ MEFs pools by double immunofluorescence staining with anti-CD147 antibody (*green*) and antibody against GM130 (*cis*-Golgi) or cadherin (cell surface) (*red*). The *right panels* represent image overlays. *Scale bar* = 10 μm. These images are representative of two independent experiments, and similar results were observed in analysis of $NCT^{-/-}$ MEFs.

Assay for Aβ-degrading Metalloproteases in Culture Medium—The culture medium from either HEK293 cells or HEK293 cells stably overexpressing CD147 was incubated with metalloprotease-specific inhibitors to indirectly identify the type of Aβ-degrading metalloproteases induced by CD147. 30 μl of conditioned medium from HEKswe cells (as the source of secreted Aβ) was incubated overnight in a 37 °C incubator with 30 μl of conditioned medium from either naïve HEK293 cells or CD147-overexpressing cells. To inhibit the degradation of Aβ during the incubation, different protease inhibitors were included as indicated. The final concentrations of the inhibitors used were 10 mM 1,10-phenanthroline (Aldrich), 5 mM EDTA, 2.5 μM thiorphan (Sigma), 10 μM Nap (a kind gift from Dr. Malcolm Leissring), 100 μM actinonin, and 50 μM GM6001 (BIOMOL International). Aβ remaining intact at the end of the incubation period was analyzed by Western blotting and quantified by enzyme-linked immunosorbent assay (ELISA) following the manufacturer's protocol (Invitrogen).

Zymography Analysis of Conditioned Medium—6 μl of conditioned medium from either naïve HEK293 cells or CD147-overexpressing cells was mixed with nonreducing sample buffer and fractionated on a 7.5% SDS gel containing 0.1% gelatin. After electrophoresis, the gel was developed and stained with Coomassie Blue as described previously (29).

RESULTS

Stability of CD147 Is Not Affected in the Absence of γ-Secretase Core Components—If CD147 is a *bona fide* component of γ-secretase, one would anticipate that the behavior of the polypeptide with respect to regulated stability would be similar to that already established for other core components of the complex, *i.e.* that the stability and maturation of γ-secretase subunits are co-regulated. To examine the stability of CD147 in cells lacking PS1/PS2, we employed fibroblasts derived from $PS1^{-/-}/PS2^{-/-}$ embryos and their wild-type (WT) littermates. As reported previously (9, 12), maturation of endogenous nicastrin was impaired, and the steady-state levels of endogenous PEN-2 were significantly reduced in $PS1^{-/-}/PS2^{-/-}$ MEFs compared with WT MEFs. In contrast and for reasons that are presently not clear, endogenous CD147 levels were elevated in $PS1^{-/-}/PS2^{-/-}$ MEFs (Fig. 1*A*, *first* and *second lanes*). To address the possibility that the observed difference in the levels of CD147 may be a result of cell-to-cell variation in the MEFs analyzed, we generated stable pools of $PS1^{-/-}/PS2^{-/-}$ MEFs overexpressing human PS1 by retroviral infection. Stable expression of PS1 in $PS1^{-/-}/PS2^{-/-}$ cells restored mature glycosylation of nicastrin and stabilized PEN-2, but did not markedly affect CD147 protein levels (Fig. 1*A*, *third* and *fourth lanes*). Similarly, CD147 levels were not reduced in $NCT^{-/-}$ or $APH1ab^{-/-}$ MEFs compared with WT MEFs, as would be expected if this polypeptide were a γ-secretase component (data not shown). Thus, the stability of CD147 is not co-regulated in a manner such as PS1, nicastrin, APH1, and PEN-2, indicating that CD147 is unlikely to be an integral subunit of the γ-secretase complex.

To further confirm the above findings, we also performed co-immunoprecipitation analyses in $PS1^{-/-}/PS2^{-/-}$ MEFs. Aliquots of 1% CHAPSO lysates of $PS1^{-/-}/PS2^{-/-}$ MEFs stably overexpressing human PS1 were immunoprecipitated with the PS1 N-terminal antiserum $PS1_{NT}$. The resulting immune complexes were subjected to Western blot analysis with anti-

CD147 antibody. The blots were then sequentially reprobed with antibodies against nicastrin, PEN-2, and PS1 CTFs. The results show efficient co-immunoprecipitation of endogenous γ-secretase core components nicastrin and PEN-2 with human PS1 expressed in $PS1^{-/-}/PS2^{-/-}$ MEFs (Fig. 1*B*). In contrast, CD147 failed to co-immunoprecipitate with PS1, nicastrin, and PEN-2 under these conditions (Fig. 1*B*). Thus, we conclude that CD147 is not a stoichiometric subunit of the γ-secretase complex.

Subcellular Localization of CD147 Is Unaffected by the Absence of γ-Secretase Core Components—Several studies have demonstrated that the integral components of γ-secretase cooperatively mature and exit the ER. CD147 is a type I membrane protein that is principally localized to the cell surface (30). To examine the subcellular localization of CD147 in the absence of γ-secretase core components, we performed confocal microscopic analysis of CD147 in $PS1^{-/-}/PS2^{-/-}$ and $NCT^{-/-}$ MEFs. There was no observable difference in the overall distribution of CD147 between $PS1^{-/-}/PS2^{-/-}$ MEFs and those expressing human PS1. Co-staining with organelle markers GM130, a *cis*-Golgi-associated protein, and cadherin, a cell-surface protein, showed similar CD147 localization in the Golgi and at the cell surface (Fig. 1*C*). Similar results were obtained in $NCT^{-/-}$ cells (data not shown). Thus, the subcellular localization of CD147 is not dependent on the expression of PS1 or nicastrin.

DRM Association of CD147 and the Core Components of the γ-Secretase Complex Is Not Codependent—We and others (27, 31) have reported that the PS1 NTF and CTF, mature nicastrin, APH1, and PEN-2 are localized within detergent-insoluble membrane microdomains, which are enriched in the lipid raft markers flotillin-2 and prion protein. Interestingly, we found that the assembly of core components precedes DRM association of the γ-secretase complex. For example, in $NCT^{-/-}$ fibroblasts, the low levels of APH1 and PEN-2 that escape degradation reside in non-raft domains (27). Therefore, we investigated whether DRM association of CD147 is dependent on the presence of γ-secretase complex components. To this end, we analyzed DRM association of CD147 in $PS1^{-/-}/PS2^{-/-}$ and $NCT^{-/-}$ MEFs and compared these profiles with that of either WT MEFs or $NCT^{-/-}$ MEFs stably overexpressing nicastrin, respectively. By sucrose density gradient fractionation, we found that CD147 was enriched in Lubrol WX-resistant membrane fractions of WT MEFs (Fig. 2*A*). However, DRM association of CD147 was unchanged in $PS1^{-/-}/PS2^{-/-}$ and $NCT^{-/-}$ cells (Fig. 2). Thus, expression of γ-secretase subunits does not regulate lipid raft association of CD147.

Several lines of evidence in cell culture and mouse brain indicate that lipid raft microdomains are the principal sites of amyloidogenic processing of APP (26, 31). Therefore, we considered the possibility that the levels of CD147 might affect the association of PS1 with DRMs and thereby influence APP processing in lipid rafts. To address this issue, we prepared membranes from HEK293 cells with different levels of CD147 expression. We observed that neither elevated nor lowered expression of CD147 had a discernible effect on the DRM association of endogenous PS1 (Fig. 3). Thus, we find it implausible that CD147 modulates lipid raft localization of γ-secretase.

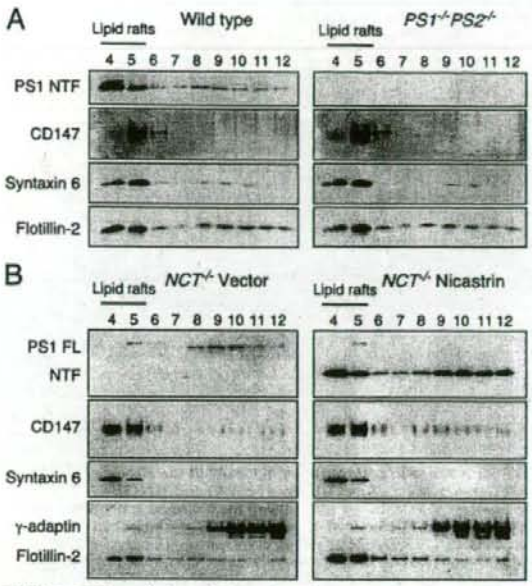

FIGURE 2. **DRM association of CD147 is not dependent on the presence of γ-secretase core components.** *A*, WT and $PS1^{-/-}/PS2^{-/-}$ MEFs were solubilized in 0.5% Lubrol WX at 4 °C for 30 min. The lysates were then subjected to flotation centrifugation on discontinuous sucrose gradients as described previously (27). The gradients were harvested from the top (fractions 1–12; top to bottom), and the distribution of PS1, CD147, syntaxin-6, and flotillin-2 was determined by fractionating 60-μl aliquots of gradient fractions 4–12. *B*, $NCT^{-/-}$ MEFs stably infected with retrovirus harboring empty vector or WT nicastrin cDNA were lysed and fractionated as described above. Note that fractions 1–3 contained no detectable signal for any protein analyzed. The raft marker flotillin-2 was recovered primarily in fractions 4 and 5, and the non-raft protein γ-adaptin was recovered in detergent-soluble fractions 9–12. The data are representative of two independent experiments; moreover, DRM fractionation was performed in WT, $NCT^{-/-}$, and $APH1ab^{-/-}$ MEFs with similar results. *FL*, full-length.

Postnatal Expression and Distribution of CD147 in Brain Show Lack of Correlation with Nicastrin—Our failure to document that CD147 levels, subcellular localization, and DRM association are co-regulated by the core components of γ-secretase in cultured cells was perplexing and prompted us to assess the expression patterns of CD147 in brain, arguably a more relevant setting. Unfortunately, little information is available pertaining to CD147 expression in brain, and hence, we sought to characterize the expression profile of CD147 relative to the γ-secretase core components PS1 and nicastrin in mouse brain during postnatal developmental stages. Western blot analyses of total brain lysates showed that CD147 protein levels were remarkably low at embryonic day 15, but readily detectable at birth. CD147 expression increased by 3.5-fold between postnatal days 0 and 7 and remained at this high level through 12 months of age (Fig. 4, *A* and *B*). A completely different expression pattern was observed for the γ-secretase core components PS1 and nicastrin, with high levels of expression occurring between embryonic day 15 and postnatal day 7 and then gradually declining after postnatal day 14 (Fig. 4, *A* and *B*). These results reveal that the developmental expression patterns

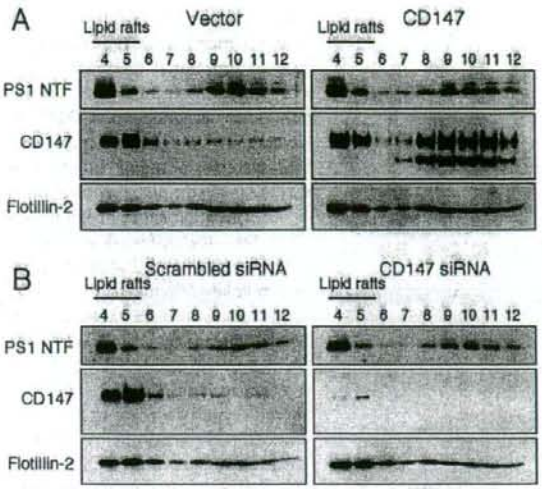

FIGURE 3. **DRM association of PS1 is not affected by CD147 overexpression or depletion.** *A*, HEK293 cells transfected with an empty vector and stably transfected cells overexpressing CD147 were lysed in 0.5% Lubrol WX and analyzed by flotation on sucrose gradients. Lipid raft localization of CD147, PS1 NTF, and flotillin-2 was analyzed by Western blotting. *B*, HEK293 cells transfected with CD147 or scrambled siRNA were fractionated as described above to analyze DRM distribution of PS1 and CD147.

of the γ-secretase core components PS1 and nicastrin do not correlate with that of CD147.

Next, we also observed remarkable differences in the cellular distributions of nicastrin and CD147 in adult mouse brain using immunohistochemical staining. We found that nicastrin immunoreactivity was restricted mainly to neuronal cell bodies throughout the cortex and to pyramidal as well as granule cells in the hippocampus (Fig. 4*C*). CD147 immunoreactivity was excluded from neuronal cell bodies, and punctate CD147 staining was seen mainly in neuronal processes. Intense CD147 staining was observed in the CA1 region of the hippocampus and upper layers of the cortex, whereas CA2 was only weakly labeled, and the dentate gyrus region was not labeled (Fig. 4*C*). The striking difference in CD147 immunoreactivity at the junction of the CA1 and CA2 regions was reproducible in all sections examined from multiple animals. The mutually exclusive pattern of nicastrin and CD147 distribution was particularly obvious in the pyramidal cell layer of the hippocampus, where nicastrin was found in the cell body and CD147 immunoreactivity was found largely in the neuronal processes within the stratum oriens, stratum radiatum, and stratum lacunosum-moleculare (Fig. 4*E*). These results do not exclude the possibility of an interaction between CD147 and γ-secretase components present at low levels in neuronal processes, but strongly suggest that CD147 is involved mainly in functions other than the regulation of the γ-secretase complex in neurons.

CD147 Depletion Increases Extracellular Aβ Independent of α- and β-Secretase Processing of APP—Consistent with the report by Zhou *et al.* (16), transfection of CD147 siRNA at increasing concentrations revealed a dose-dependent increase in Aβ levels in the medium of HEK293 cells transiently overexpressing human WT APP695 (Fig. 5*A*). In these studies, we found no significant change in the levels of full-length APP, APP CTFs, or secreted APPα (Fig. 5*A*) These results suggest that the increase in secreted Aβ associated with the depletion of CD147 expression is independent of α- and β-secretase processing of APP. To confirm these data, we analyzed the effect of siRNA-mediated knockdown of CD147 expression on secreted Aβ levels in cells stably expressing APPswe. We observed a small but consistent increase in secreted Aβ levels in cells transfected with CD147 siRNA compared with those transfected with control siRNA, whereas the steady-state levels of α- and β-CTFs remained unchanged (Fig. 5*B*). Taken together, these results indicate that siRNA-mediated depletion of CD147 expression increases the levels of Aβ in medium without significant changes in the levels of APP CTFs, the penultimate substrates of γ-secretase, hence arguing against an effect on β- or α-secretase processing of full-length APP.

In addition to the extracellular release of Aβ, γ-secretase cleavage of APP CTFs at the "ε-site" releases the APP intracellular domain (AICD) from the membrane. Similarly, ε-cleavage of Notch releases the Notch intracellular domain (NICD). To examine the potential influence of CD147 on ε-cleavage of substrates, we first asked whether depletion of CD147 has any effect on AICD production. We found that there was no quantitative difference in the levels of AICD generated by cleavage of C-terminally epitope-tagged APP (APP695-6Myc) in transfected HEK293 cells following siRNA-mediated depletion of CD147 expression (Fig. 5*C*). Furthermore, CD147 depletion had no discernible effect on the generation of the NICD following γ-secretase cleavage of N-terminally truncated Notch (mNotchΔE) at the ε-site (Fig. 5*D*). Pretreatment of transfected cells with Compound E markedly diminished the production of the AICD and NICD, establishing the specificity of these commonly used cell-based γ-secretase assays. Thus, we conclude that CD147 does not modulate ε-cleavage of substrates by the γ-secretase.

CD147 Effect on Aβ Levels Is Not Mediated through Direct Modulation of γ-Secretase Activity—CD147 has been implicated in many cellular functions, including the induction of MMPs (18) and cell-surface trafficking of the monocarboxylate transporters MCT1 and MCT4 (32). Therefore, we asked whether the influence of CD147 on extracellular Aβ levels could be mediated through direct modulation of γ-secretase, as was reported previously (16), or by an indirect mechanism unrelated to γ-secretase processing of APP β-CTFs. To this end, we asked whether we could recapitulate the cell-based findings of a role for CD147 in Aβ production in a well established *in vitro* reconstitution system that employs detergent-solubilized membranes in conjunction with a purified C100 substrate (14). The rationale for using the *in vitro* assay is that it selectively reports on Aβ production by γ-secretase cleavage of recombinant C100-FLAG substrate, thereby formally ruling out the potential influence of CD147 on trafficking of APP or the β-CTF, exocytosis or endocytosis of Aβ, and stability of extracellular Aβ, which might account for the increase in Aβ levels in the conditioned medium of CD147-depleted cells observed in both our experiments and the earlier study. As an internal control for the enzyme selectivity in this *in vitro* assay, we incubated parallel reactions with L685,458, a potent transi-

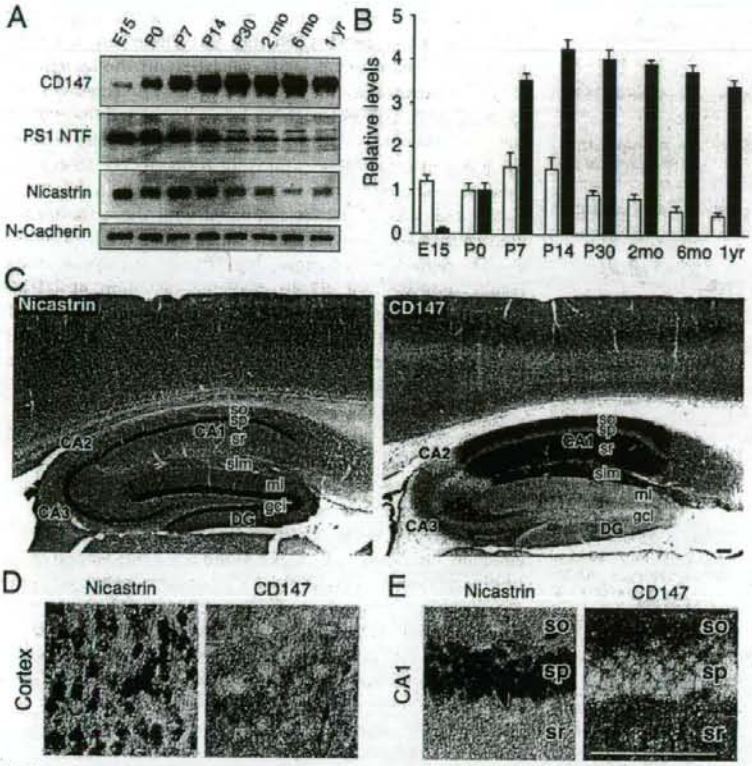

FIGURE 4. **Uncorrelated protein expression profile between CD147 and γ-secretase integral components in mouse brain.** *A*, lysates from mouse brains harvested at the indicated stages of embryonic (*E*), postnatal (*P*), and adult development were analyzed by immunoblotting. *mo*, month; *yr*, year. *B*, signal intensities of CD147 and nicastrin were determined from three independent samples and normalized to N-cadherin levels. For comparison, the normalized expression level of each protein at postnatal day 0 was set to 1, and the level of expression relative to postnatal day 0 was plotted. *C*, shown is the immunocytochemistry for nicastrin and CD147 in the hippocampus and overlying cortex of 2-month-old C57BL/6J mouse brain. *D* and *E*, higher magnifications are shown of the cortex and pyramidal cell layer in the CA1 region of the hippocampus. Nicastrin immunoreactivity was essentially restricted to neuronal cell bodies in the cortex and hippocampus, whereas CD147 immunoreactivity was excluded mainly from the cell bodies. Intense CD147 immunoreactivity was found in the CA1 stratum oriens (*so*), stratum radiatum (*sr*), and also stratum lacunosum-moleculare (*slm*). Note that anti-CD147 antibody also labeled blood vessels. *DG*, dentate gyrus; *gcl*, granule cell layer; *ml*, molecular layer; *sp*, stratum pyramidale. *Scale bar* = 100 μm. These images are representative of two independent experiments.

tion-state isostere inhibitor of γ-secretase. Surprisingly, the *in vitro* Aβ assays revealed that membranes isolated from CD147-depleted HEK293 cells did not increase Aβ production compared with those of control siRNA (Fig. 5*E*). Compared with the obvious increase in extracellular Aβ levels followed by CD147 depletion in intact cells, the results obtained from *in vitro* Aβ assays were unanticipated. The above results strongly suggest that the regulatory function of CD147 on extracellular Aβ levels is unlikely mediated through its proposed role as a regulatory subunit of the γ-secretase complex, which modulates intramembranous proteolysis of substrates.

Reduced Stability of Synthetic Aβ in Medium Conditioned by HEK293 Cells Overexpressing CD147—The series of preceding experiments failed to confirm the proposal that CD147 plays a role in Aβ production by modulating γ-secretase levels and activity. Hence, we were left with the scenario that CD147 modulates extracellular Aβ levels via an indirect mechanism that engages a known functional attribute of the polypeptide. Among the diverse functions assigned to CD147 in diverse physiological and pathological systems, a major function of CD147 is to stimulate production of a set of MMPs, some of which are shed into the extracellular space. Thus, we reasoned that MMPs that are regulated/induced by CD147 might modulate extracellular Aβ levels. To address this possibility, we generated stable HEK293 cells overexpressing CD147 and observed a small decrease in Aβ in the conditioned medium compared with that of parental HEK293 cells (Fig. 6*A*). As we had predicted based on siRNA studies, overexpression of CD147 had no effect on the levels of AICD or NICD production in cells transfected with APP695-6Myc or mNotchΔE, respectively (Fig. 6, *B* and *C*).

To investigate whether the observed decrease in extracellular levels of Aβ is mediated through CD147 induction of MMPs that are known to be capable of degrading Aβ (29, 33–36), we examined the stability of synthetic $Aβ_{40}$ and $Aβ_{42}$ peptides in the conditioned medium of HEK293 cells transfected with an empty vector or stable CD147 cells. For this assay, we incubated aliquots of conditioned medium (containing undetectable levels of endogenous Aβ) with 50 ng of synthetic $Aβ_{40}$ peptides at 37 °C overnight and performed Western blotting to detect synthetic $Aβ_{40}$ remaining in the reaction. Surprisingly, there was considerable loss of synthetic Aβ in the reactions containing culture medium from CD147-overexpressing cells compared with HEK293 cells (Fig. 7*B*). After 14 h of incubation *in vitro*, the medium conditioned by CD147-overexpressing cells degraded significantly higher levels of input Aβ (nearly 90 and 70% of input $Aβ_{40}$ and $Aβ_{42}$, respectively, by the medium of CD147 cells *versus* 60 and 50% of input $Aβ_{40}$ and $Aβ_{42}$ by the medium of naïve HEK293 cells). To further rule out any contribution of γ-secretase to extracellular degradation of synthetic Aβ potentiated by CD147 overexpression, we treated stable CD147 cells treated with the γ-secretase inhibitor Compound E prior to collecting the conditioned medium. *In vitro* Aβ degradation assays showed that the medium conditioned by stable CD147 cells degraded Aβ to the same degree regardless of the differences in their γ-secretase activity, *i.e.* treated or not

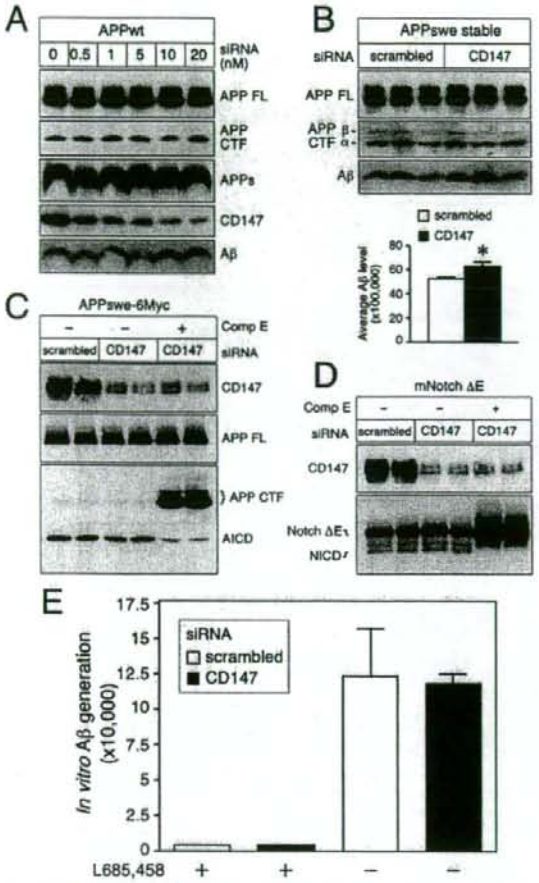

FIGURE 5. **Increase in Aβ levels associated with the depletion of CD147 is independent of APP secretase activities.** *A*, HEK293 cells were transiently transfected with increasing doses of CD147 siRNA together with WT APP695 cDNA. 50 μg of total cell lysates was analyzed by Western blotting to examine the levels of full-length (*FL*) APP, APP CTF, and CD147. The levels of secreted APP (*APPs*) and Aβ conditioned medium were analyzed by immunoblotting. *B*, HEKswe cells were transfected with scrambled or CD147 siRNA and analyzed as described above. The levels of Aβ were quantified by ELISA and plotted (mean ± S.E., $n = 3$; *, $p < 0.02$). *C*, HEK293 cells were cotransfected with either scrambled or CD147 siRNA duplex and a plasmid encoding APPswe-6Myc. Compound E (*Comp E*; 10 nM) was added as indicated to inhibit γ-secretase activity. *D*, conditions were the same as described for *C* except that cells were transfected with a plasmid encoding mNotchΔE instead of APP. *E*, membranes prepared from siRNA-treated cells were used in an *in vitro* assay to monitor γ-secretase processing of recombinant C100-FLAG substrate (14). The reactions were performed in the presence or absence of 1 μM L685,458 to establish the specificity of the assay. $Aβ_{40}$ generated by γ-secretase cleavage of the substrate was quantified by ELISA and plotted (mean ± S.E., $n = 3$).

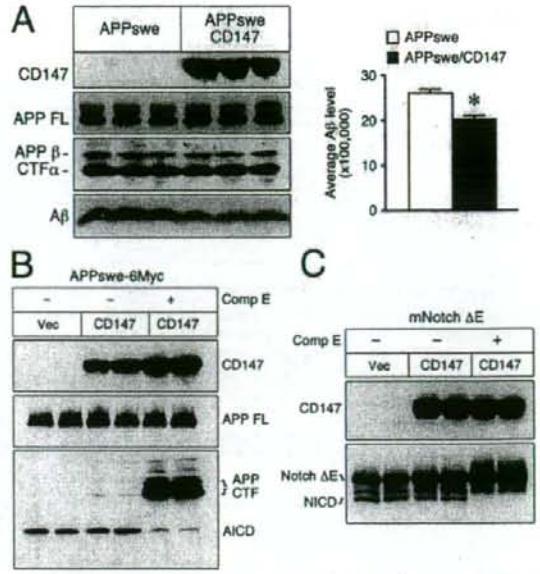

FIGURE 6. **Decrease in Aβ levels associated with CD147 overexpression is independent of APP secretase activities.** *A*, overexpression of CD147 reduces Aβ in conditioned medium. Total cell lysate and the conditioned medium from HEK293 cells stably expressing either APPswe or APPswe and Myc-tagged CD147 were used to analyze the levels of full-length (*FL*) APP and Aβ. Total Aβ levels in the conditioned medium were quantified by ELISA and plotted (mean ± S.E., $n = 3$; *, $p < 0.0005$). *B*, HEK293 cells were transiently cotransfected with an empty vector (*Vec*) or with Myc-tagged CD147 cDNA along with APPswe-6Myc. Compound E (*Comp E*; 10 nM) was added as indicated to inhibit γ-secretase activity. *C*, conditions were the same as described for *B* except that cells were transfected with a plasmid encoding mNotchΔE instead of APP. AICD and NICD experiments were repeated twice with similar results.

with Compound E (Fig. 7, *A* and *B*). Thus, CD147-mediated extracellular degradation of Aβ levels by CD147 is independent of γ-secretase activity.

A recent report has linked MMP-2 and MMP-9 to Aβ degradation (29). To examine the possibility that these two enzymes might be involved in Aβ degradation in the conditioned medium of CD147-overexpressing cells, we performed gelatin-substrate zymography (Fig. 8*A*). We failed to detect differences in the levels of MMP-2 and MMP-9 activities in the culture medium of CD147-overexpressing cells relative to that of naïve HEK293 cells. This result ruled out the contribution of these two enzymes and indicated that other protease(s) likely contribute to enhanced Aβ degradation in CD147-conditioned medium. Therefore, we mixed several metalloprotease inhibitors with the conditioned medium from CD147-overexpressing cells and then incubated these mixtures with Aβ secreted from HEKswe cells for 15 h at 37 °C (Fig. 8*B*). As a control, we used the conditioned medium from naïve HEK293 cells in the absence of inhibitors. Each of the inhibitors used in this assay showed different levels of inhibition of Aβ degradation. EDTA and 1,10-phenanthroline exhibited the highest level of inhibition, indicating metalloprotease(s) are involved in Aβ degradation. Thiorphan and Nap, a neprilysin inhibitor and an insulin-degrading enzyme inhibitor, respectively, as well as two MMP inhibitors, actinonin and GM6001, also inhibited Aβ degradation. Although these results cannot identify a single enzyme activity that is responsible for enhanced Aβ degradation in the conditioned medium of CD147-overexpressing cells, they could imply that one or more metalloproteases or MMPs are involved in this degrading activity. At present, the identity of the protease(s) in the conditioned medium of CD147-overex-

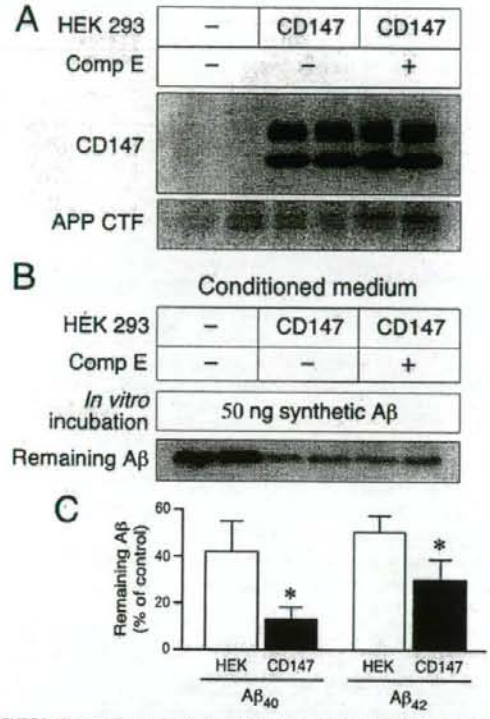

FIGURE 7. **Comparison of $A\beta_{40}$ and $A\beta_{42}$ degradation by the conditioned medium from HEK293 or HEK293 cells overexpressing CD147.** *A* and *B*, CD147 potentiation of extracellular Aβ degradation is independent of γ-secretase activity. Naïve HEK293 cells or CD147-overexpressing cells were cultured in the presence or absence of 10 nM Compound E (*Comp E*) overnight, and their conditioned media were collected. *A*, Western blots of detergent lysates show CD147 overexpression and an increase in endogenous APP CTFs by Compound E treatment. *B*, aliquots of the conditioned media were mixed with 50 ng of synthetic $A\beta_{40}$, and the mixtures were incubated at 37 °C. After a 14-h incubation, the mixtures were resolved on a Tris/Tricine gel and blotted with 26D6 to detect the remaining $A\beta_{40}$ peptides. *C*, synthetic $A\beta_{40}$ or $A\beta_{42}$ was incubated for 14 h with medium conditioned by naïve HEK293 cells or cells stably overexpressing CD147. $A\beta_{40}$ and $A\beta_{42}$ remaining intact at the end of the incubation period were quantified by Western blotting, and the percentage of Aβ remaining was calculated relative to the levels in reactions containing fresh culture medium (mean ± S.E., $n = 8$; *, $p < 0.001$).

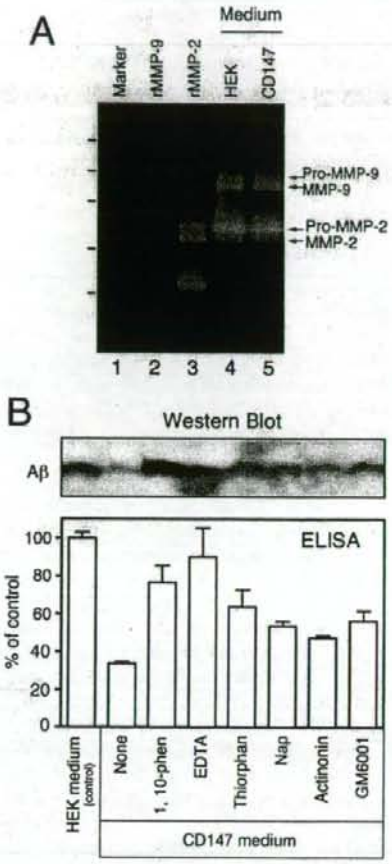

FIGURE 8. **Assays of CD147-dependent proteases that degrade Aβ in the medium.** *A*, gelatin-substrate zymography shows no difference in MMP-2 and MMP-9 activities in culture medium from CD147-overexpressing cells relative to medium conditioned by naïve HEK293 cells. *Lanes 2* and *3* contain recombinant MMP-9 and MMP-2, respectively. *B*, conditioned medium from CD147-overexpressing cells was incubated with secreted Aβ (medium from HEKswe cells) as described under "Experimental Procedures" in the presence or absence of different protease inhibitors. The conditioned medium from naïve HEK293 cells was used as a control in the absence of protease inhibitor. The levels of remaining Aβ were either visualized by Western blotting or quantified by ELISA and plotted. Note that for unknown reason, the levels of Aβ in medium containing 1,10-phenanthroline (*1,10-phen*) were consistently underestimated by ELISA. These experiments were repeated three times.

pressing cells is elusive, but it remains an active subject of investigation.

DISCUSSION

CD147 was previously identified as a protein associated with γ-secretase complex in detergent-solubilized HeLa cell membranes (16). These earlier studies revealed that siRNA knockdown of CD147 caused a dose-dependent increase in secreted Aβ levels. Remarkably, the mechanism(s) by which CD147 expression modulated extracellular Aβ levels were not determined at the time of publication, and information has not emerged in the interim in this regard. In this study, we have provided a detailed examination of the potential regulatory role of CD147 in the γ-secretase complex and now offer several novel insights. First, we have provided several lines of *in vitro* and *in vivo* evidence to suggest that CD147 expression, stability, and localization are regulated independently of the core subunits of γ-secretase. Furthermore, we failed to observe a detectable interaction between CD147 and γ-secretase complex subunits using a co-immunoprecipitation condition widely used by several groups to immunoaffinity purify the active γ-secretase complex (for example, see Ref. 14). Second, although we confirmed that depletion of CD147 in a human cell line modulates extracellular Aβ levels similarly as reported previously in Chinese hamster ovary cells (16), we failed to demonstrate that CD147 modulates Aβ production in an *in vitro* γ-secretase reconstitution assay. Moreover, we have shown that overexpression or depletion of CD147 expression failed to affect AICD